JOURNAL OF GEOPHYSICAL RESEARCH, VOL. 99, NO. B11, PAGES 22,059–22,086, NOVEMBER 10, 1994

Viscosity estimates for the crust and upper mantle from patterns of lacustrine shoreline deformation in the Eastern Great Basin

Bruce G. Bills, [1,2] Donald R. Currey, [3] and Grant A. Marshall[4]

Abstract. The deformed shorelines of Lake Bonneville constitute a classic source of information on lithospheric elastic thickness and upper mantle viscosity. We describe and apply a new model to a recently augmented data set. New data better constrain both the complex spatio-temporal pattern of the lake load and the crustal deformation response to that load. The history of lake level fluctuations has been significantly refined and somewhat modified. This is due to both more radiocarbon dates from within the Bonneville basin and to an improved calibration of the radiocarbon timescale itself. The data which constrain the crustal deformation pattern consist of ages and shoreline elevations from several hundred points which sample three major levels of Lake Bonneville and corresponding elevations from the high stands of three smaller lakes situated to the west of Lake Bonneville. The data from the smaller lakes help elucidate the pattern of deflection which occurred beyond the edge of the big lake. The geometry of the Earth model incorporates an arbitrary number of layers overlying a half-space, and the rheology of each level can accommodate an arbitrary number of Maxwell viscoelastic elements in parallel. The inverse modeling comprises three complementary approaches: for the simplest configurations, we performed a direct search of the parameter space and delineated the irregular boundary of the subspace of acceptable models. For more complex configurations, we constrained the elastic parameters to their seismically determined values and then solved for viscosity versus depth profiles by either expressing the log(viscosity) versus log(depth) profile as a series of specially constructed orthogonal polynomials, or by allowing each of 8-10 layers (plus the half-space) to have an independently determined viscosity. We found that the data do not strongly support (nor can they conclusively exclude) a more complex rheology than simple Maxwell viscoelasticity. The orthogonal polynomial solution exhibits an essentially monotonic decrease in viscosity with depth. The most rapid change occurs at shallow depths, decreasing from 10^{23} Pa s at 3 km to 10^{20} Pa s at 30 km. The decrease is much more gradual below, with only another factor of 5 decrease between 30 and 300 km depth. The unconstrained solution exhibits a rapid decrease in viscosity with depth from 2×10^{24} Pa s in the top 10 km to 4×10^{17} Pa s at a depth of 40 km. A nearly isoviscous asthenospheric region extends from 40 to 150 km and is underlain by a mantle lithospheric region with increased viscosity (2×10^{20} Pa s) extending from 150 to 300 km depth and by a uniform viscosity (10^{19} Pa s) half-space below.

Introduction

Climatically forced oscillations in the depth and areal extent of numerous lakes throughout the Eastern Great Basin provide a natural laboratory for investigating Earth's response to normal loads on spatial scales of tens to thousands of kilometers, and time scales of decades to millennia. Lake Bonneville was the largest of the late Pleistocene pluvial lakes in the Great Basin, attaining a maximum depth of 380 m and an areal extent of 52,000 km^2. Under a load of that size, the crust was deflected downward by 60-70 m. As the lake surface elevation stabilized at various levels, individual shorelines were formed on horizontal (equipotential) surfaces. After the Bonneville load was removed, the crust rebounded, and present departures from horizontality of these paleoshorelines thus provide a valuable source of information concerning viscosity variations within the crust and upper mantle. Several smaller lakes occupied basins to the west of Bonneville. They were generally too small to produce appreciable deflection, but their shorelines record the far-field portion of the Bonneville

[1]Geodynamics Branch, NASA Goddard Space Flight Center, Greenbelt, Maryland.

[2]Department of Earth and Planetary Sciences, Johns Hopkins University, Baltimore, Maryland.

[3]Limneotectonics Laboratory, Department of Geography, University of Utah, Salt Lake City.

[4]Branch of Earthquake Geology and Geophysics, U.S. Geological Survey, Menlo Park, California.

Paper number 94JB01192.
0148-0227/94/94JB-01192$05.00

response. Though the deflection patterns of Lake Bonneville shorelines have been analyzed many times in the past, acquisition of new data, recent revisions in the radiocarbon time scale calibration, and implementation of an improved computational model prompt us to revisit this problem.

Previous Work

The scientific investigation of Lake Bonneville began with the classic work of *Gilbert* [1890]. In the course of a reconnaissance survey of shoreline deposits of the Bonneville basin, he discovered that the shorelines in the center of the basin were at higher elevations than their counterparts on the basin periphery. He initially considered several hypotheses to explain this observation but eventually settled on the notion that the load of the lake waters had depressed the Earth's crust downward by some tens of meters, the shorelines had formed as level surfaces on the depressed landscape, and, upon removal of the load, the crust had rebounded to its present configuration. He also recognized that the amount of rebound was less than would be expected on purely buoyant support and calculated that an Earth model consisting of an elastic plate 50 km thick over a dense but inviscid fluid would have the required response. This is apparently the earliest published empirical estimate of what would now be termed an elastic lithospheric thickness. He also considered the possibility of viscous or plastic flow in the underlying regions but conceded that too little was known at the time about the elastic properties of rocks to make quantitative estimates of their departures from perfect elasticity. *Gilbert* [1890, p.383] concluded his discussion of these observations with the prescient comment:

> The application of an analytic theory of these relations could yield the best results only with a better determination than we now have of the elasticities of rocks, and with a better determination of the figure of the deformation of the Bonneville Basin; but even with the imperfect data at hand it might establish a presumption for or against the existence of a liquid substratum beneath the rigid crust, and if the mathematical difficulties were surmounted, there can be little question that the observational data would be supplied, for their procurement is opposed by little beside their expense.

Since that time, significant progress has been made on both the observational and theoretical fronts. Critical observations are of two types: patterns of shoreline deflection and constraints on lake elevation history. *Gilbert* [1890] presented elevation measurements for 33 points on the Bonneville shoreline, and 12 points on the Provo shoreline. *Crittenden* [1963a,b] measured elevations of 90 points on the Bonneville shoreline, and *Passey* [1981] measured 24 points each on the Bonneville and Provo shorelines. *Currey* [1982] has compiled the most complete and well documented set of shoreline elevation measurements, including 181 point elevations on the Bonneville shoreline, 112 on the Provo shoreline, and 48 on the Gilbert shoreline. These measurements were the basis for the analysis of *Bills and May* [1987], and constitute a major component of the present study.

Gilbert [1890] had no way of reliably estimating absolute ages of the various shoreline features he saw, but he did surmise that the high stand of the lake was broadly contemporaneous with the last major glaciation. He also worked out a relative chronology which is closely supported by more recent work. The lake stage sequence of *Morrison* [1965, 1966] was used in many of the modeling efforts during the 1970s and 1980s. However, recent work has significantly modified the absolute chronology of the early deep-lake cycles, and has added important structural detail the last deep-lake cycle. *Currey* [1990] has presented a review of current understanding of the lake history, including important contributions by *Eardley et al.* [1973], *Scott et al.* [1983], *Spencer et al.* [1984], *Currey et al.* [1983, 1984], and *Currey and Oviatt* [1985]. That chronology represents current consensus on the last deep-lake cycle and is adopted as definitive in the present study. *Morrison's* [1991] recent work agrees quite well with this chronology prior to 14 ka but is very different during the latter stages, with a reexpansion to the Provo level at ~10 ka.

Nakiboglu and Lambeck [1982] give a reasonably complete review of Bonneville modeling studies prior to their own work. Earlier work includes efforts by *Gilbert* [1890], *Crittenden* [1963a,b, 1970], *Brotchie and Sylvester* [1969], *Walcott* [1970], *Cathles* [1975], and *Passey* [1981]. Subsequent, but similar efforts were by *Nakiboglu and Lambeck* [1983], *Bills and May* [1987] and *May et al.* [1991]. Though these investigations differed in detail, all were essentially employing a similar Earth model, which basically consists of a thin elastic plate over a Maxwell half-space.

Iwasaki and Matsu'ura [1982] were apparently the first to use a more realistic Earth model, consisting of multiple viscoelastic layers over a Maxwell half-space. Though the model could have an arbitrary number of layers, they concluded that the data did not support any more complexity than had been exhibited in earlier generations of models. They estimated that the elastic lithosphere is 30-40 km thick, and the viscosity of the substrate is $1\text{-}2\times10^{20}$ Pa s. However, their failure to resolve more structure is mostly due to the fact that they used an extremely simplified spatio-temporal representation of the load and only compared their model with the pattern revealed by *Crittenden's* [1963a,b] Bonneville elevation data. As we will see in later sections, the data do support more detailed inferences.

Advantages of Lake Loads

Much of what is known about the rheology of Earth's deep interior has been inferred from modeling vertical motions caused by waxing and waning of ice sheets and recorded by marine shorelines. Obvious advantages of glacial loads versus lacustrine loads are their larger amplitude (several thousand meter ice thickness, compared to several hundred meter water depth) and sufficient lateral extent (thousands of kilometers versus hundreds of kilometers) to excite flow at considerable depth. The chief disadvantage of the glacial rebound process as a probe of Earth rheology is that the load is not as well known. In fact, a difficult (and perhaps nonunique) inverse problem must be solved just to determine the glacial load, whereas the lacustrine load can be much more readily determined. The reason for this is simple; the top surface of a lake is an equipotential surface. Knowledge of present-day topography and a history of lake surface elevation through time suffices to trivially reconstruct the spatio-temporal pattern of lake loads to within a few percent accuracy, whereas similar accuracy glacial load reconstructions are fraught with difficulty and may not even be attainable. Furthermore, lakes are much better recorders of climatic history than are glaciers and ice sheets [*Currey*, 1990].

Motivation for Present Study

The data used in our previous analysis [*Bills and May*, 1987] consisted of present elevations of several hundred points well distributed around the basin on the highest element of the Bonneville (1550 m), Provo (1440 m), and Gilbert (1300 m) shoreline complexes (Currey, 1982). The locations and elevations of these points are available as electronic supplement[1] Tables A1, A2, and A3, respectively. The new data included in the present analysis are of several types. The history of lake level fluctuations has been significantly refined and somewhat modified [*Currey and Oviatt*, 1985; *Currey*, 1990]. The Bonneville and Provo shoreline complexes comprise nine and seven morphologically distinctive threshold-controlled stages, respectively [*Currey and Burr*, 1988]. The Bonneville and Provo data sets used in our previous modeling efforts correspond to B5 (15.0 ka, 181 locations) and P3 (14.3 ka, 121 locations), respectively. At a few locations, the time dependence of the deflection is well constrained, as the elevations of shorelines corresponding to all 16 of these distinct stages are now known [*Burr and Currey*, 1988].

An additional new data set consists of elevations at a number of points on the highest shorelines of three smaller lakes situated to the west of Lake Bonneville,

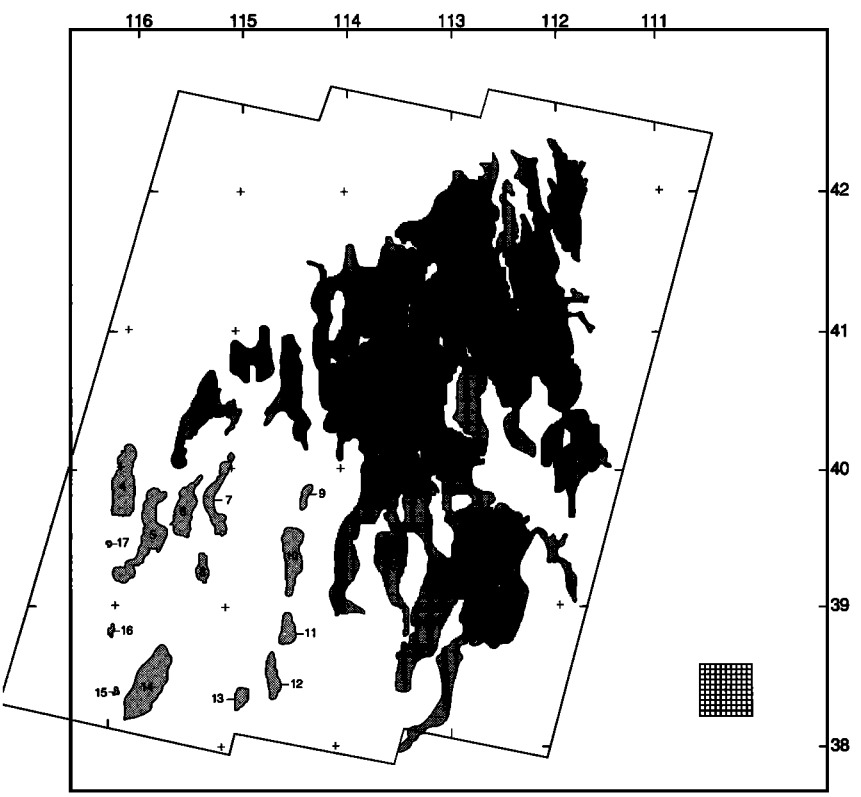

Figure 1. Late Pleistocene lakes: Eastern Great Basin. Numbers associated with lakes correspond to listing in Table 1. The large square represents the central 600×600 km of the 1024×1024 km area used in the deflection calculations. This same square appears as the boundary of the remaining map view figures (Figures 2-4 and 14-18). Small square in lower right shows example of 4×4 km grid cells. The irregular outline corresponds to the shape of a Landsat image mosaic of the study area presented by *Bills and May* [1987].

at distances of 10-50 km (Lake Waring, 50 points), 30-70 km (Lake Clover, 27 points), and 60-120 km (Lake Franklin, 43 points). These measurements help elucidate the pattern of deflection which occurred beyond the edge of the large lake at a time close to that of the highest Bonneville shoreline. Figure 1 illustrates the shapes and locations of these, and other small lakes, relative to Lake Bonneville. As is indicated in Table 1, all of these peripheral lakes were very much smaller than Bonneville. Electronic supplement Tables A4, A5 and A6 list the locations and elevations of the peripheral lake shoreline points used in the present study. The Lake Waring elevations are from *Currey et al.*, [1984]. The Lake Clover and Lake Franklin data represent new field measurements. The pattern of shoreline deflection indicated by those measurements is similar to that seen by *May et al.* [1991] using spot elevations taken from topographic maps of the region. Figures 2-4 give various views of the deflection pattern reflected in these data. A constant value has been subtracted from each of the Waring, Clover, and Franklin reference surfaces (187, 157, and 287 m, respectively) to make them concordant with the Bonneville data. Finding the appropriate constant value for each lake basin is a part of the modeling process.

The Great Basin lacustrine histories are based primarily on ^{14}C dates. Until recently, there was no reliable calibration of the radiocarbon time scale prior to 10 ka. The recent work of *Bard et al.* [1990], which compared U/Th versus C dates for corals near Barbados, has extended that calibration back to 30 ka. Though the calibration curve is nonlinear, the dominant effect, over the interval of primary interest to the Bonneville basin loading history, is a 16 percent increase in the time scale. This calibration has been widely used to obtain improved chronologies of lacustrine and marine level fluctuations [*Tushingham and Peltier*, 1991,1993; *Toscano and York*, 1992; *Yechieli et al.*, 1993]. Figure 5 shows lake level fluctuation curves of *Currey* [1990], with and without application of the new calibration. The calibrated curve is used, with minor modification, in our modeling.

In previously published analyses of the Bonneville shoreline data [*Crittenden*, 1963a,b; *Nakiboglu and Lambeck*, 1983; *Bills and May*, 1987], the Earth model had, at most, only two significant parameters: thickness of an elastic lithosphere and effective viscosity of an upper mantle region with Maxwell rheology. The deflection model used in the present analysis has some features in common with the earlier version employed by *Bills and May* [1987]: the water load is determined from a 4×4 km topography array and a piecewise linear approximation to the lake level history. The spatial and temporal load variations are Fourier and Laplace transformed, a filter appropriate to the selected Earth model is applied, and the response is back transformed to the spatial/temporal domain for comparison with the data. The major improvement in the new model is the incorporation of a quasi-static propagator matrix formulation in the calculation of the filters. This allows inclusion of an arbitrary number of layers in the Earth model. The rheology of each layer is specified by an arbitrary number of Maxwell elements in parallel. We have found, however, that the present data do not generally warrant use of more than a single element in each layer. The elastic parameters are assumed known from seismic studies [*Priestley et al.*, 1980].

The propagator matrix formulation (as presently implemented) requires that the material properties be constant throughout each layer. Complex vertical struc-

Table 1. Late Pleistocene Lakes of the Eastern Great Basin

	Valley	Lake	Area km^2	Depth m	Volume km^3
		Bonneville	51,300	380	9500
1	Goshute	Waring	2640	30	40
2	Clover	Clover	1400	60	40
3	Ruby	Franklin	1250	25	40
4	Diamond	Diamond	1010	70	35
5	Newark	Newark	780	70	28
6	Long	Hubbs	510	74	18
7	Butte	Gale	410	28	5.5
8	Jakes	Jakes	160	26	2.1
9	Antelope	Antelope	120	24	1.4
10	Spring	Spring	600	74	22
11	Spring	Maxey	210	40	4.1
12	Lake	Carpenter	350	20	3.7
13	Cave	Cave	180	30	2.7
14	Railroad	Railroad	970	50	24
15	Sand Spring	Lunar	16.3	4	0.03
16	Little Smoky	Corral	23.6	–	–
17	Stevens	Yahoo	5.1	34	0.09

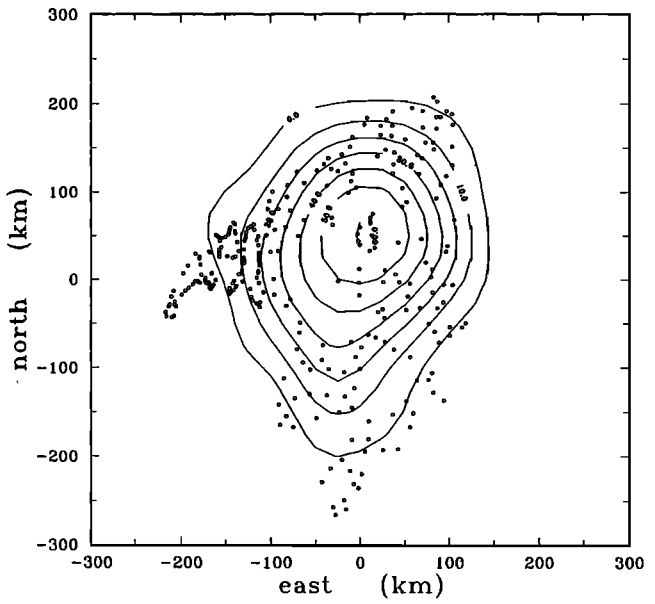

Figure 2a. Observed deflection pattern for Bonneville epoch. Map View. Small circles indicate survey locations. Contours indicate excess elevation relative to 1558.9 m in Bonneville basin. Points in Waring, Clover, and Franklin basins have reference elevations of 1750.6, 1722.7 and 1854.0 m, respectively. Lateral positions are given in kilometers east and north of an arbitrary reference position with Universal Transverse Mercator (UTM zone 12) coordinates of (easting = 33^{0000}, northing=448^{5000}). This position corresponds to 40.50°N, 113.00°W. The edges of this figure correspond to the large square in Figure 1.

tures can be approximated by including a large number of layers. Early experiments with inverse models allowed an independent viscosity value in each of several (up to 10) layers. Interesting, but largely spurious, structures appeared in those models. A preferable approach specifies the values of elastic properties (density, shear modulus, and Lame's constant) from the model of *Priestley et al.* [1980] in each of 29 layers and solves for a smooth viscosity profile. Smoothness is ensured by representing the log(viscosity) versus log(depth) variations in terms of a small number (2-6) of orthogonal polynomials down to some cut-off depth and then imposing a constant viscosity below that depth.

Deflection Model

Before we can estimate Earth model parameters from the observed spatio-temporal deflection field, we need a forward modeling capability with which to compute the vertical and lateral deflections expected for a given Earth model, subjected to specified normal loads. Our approach is to start by computing the surface displacements due to applied normal loads in a transversely isotropic, compressible, linearly elastic medium. As the inertial terms in the force balance are neglected, the elastic solutions obtained are strictly static. However, the quasi-static response of viscoelastic models to time dependent loads can be obtained from these same solutions via a Laplace transformation of the time variable. Our solution to this viscoelastic displacement problem is similar to that presented by several previous workers [*Singh*, 1970, 1986; *Rundle*, 1978, 1980, 1982; *Ward*, 1984, 1985; *Pan*, 1989], and details of our algorithm are presented in electronic supplements Appendices B and C. We simply summarize the objectives and results of the analysis; details of the derivations are given by the above references.

Elastic Model

At the wavelengths appropriate to this problem, the perturbations to the stress field and the gravity field

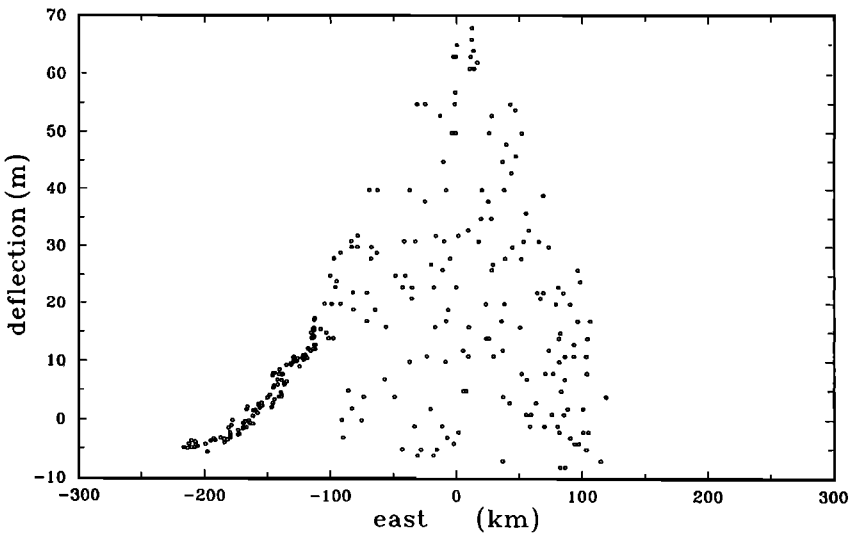

Figure 2b. East-west projection for Bonneville epoch. The same elevation data as in Figure 2a are projected onto an east-west oriented plane. The cluster of points on the western margin are from Lakes Waring, Clover, and Franklin.

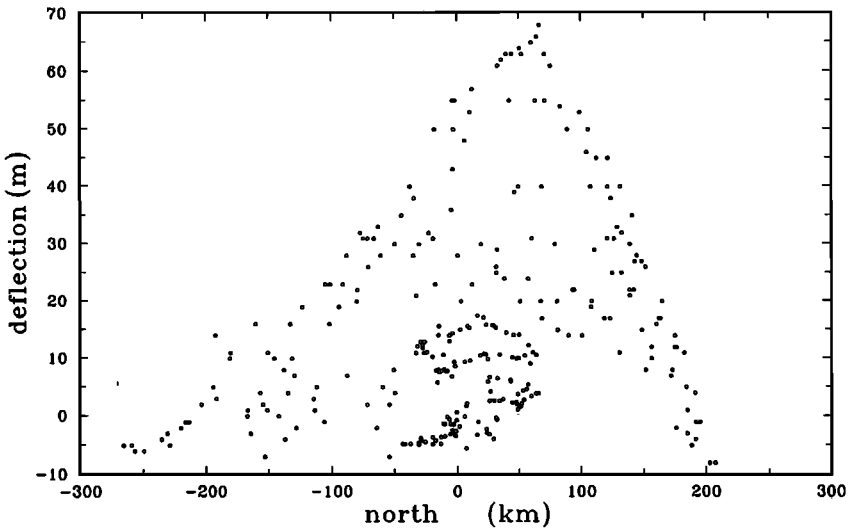

Figure 2c. North-south projection for Bonneville epoch. The same elevation data as in Figure 2b are projected onto a north-south oriented plane.

that are induced by the loading are effectively decoupled. Associated with an arbitrary water depth distribution, $d(x_1, x_2)$ is a normal load

$$t_{zz}(x_1, x_2, 0) = -\rho_w \, g \, d(x_1, x_2), \tag{1}$$

where ρ_w and g are the density of water and the gravitational acceleration, respectively. In the substrate, the elastic stresses t_{ij} are related to the displacements u_i via a linear constitutive relation

$$t_{ij} = \lambda \, \delta_{ij} u_{k,k} + \mu(u_{i,j} + u_{j,i}), \tag{2}$$

where λ and μ are the Lame constants. Several options are available for combining gravitational and elastic forces in the calculation of load induced flexure of elastic Earth models. One approach is to modify the elastic boundary conditions to include a buoyancy term. This technique was used, for example, by *McConell* [1965] and *Nakiboglu and Lambeck* [1982]. Another approach, developed by *Love* [1911] and advocated by *Wu and Peltier* [1982] and *Wolf* [1985a,b], includes a prestress advection term in the momentum balance. Our approach follows the latter pattern. The stresses associated with the load are balanced by a combination of elastic and buoyancy effects

$$\frac{\partial(t_{ij} + \rho \, g \, u_3)}{\partial x_j} = 0. \tag{3}$$

After applying a horizontal wavenumber transformation (either a Fourier transform for Cartesian coordinates or a Hankel transform for cylindrical coordinates), equations (2) and (3) can be combined into a single matrix equation of the form

$$\frac{df(k, z)}{dz} = M(k, z) f(k, z), \tag{4}$$

where k is the spatial transform variable. We will find it convenient to partition the vector

$$f = [U; T]^t, \tag{5}$$

where U is a vector of displacements and T is a vector of stresses. In cylindrical and Cartesian coordinates it takes the explicit forms

$$f = [u_r, \, u_z; \, t_{rz}, \, t_{zz}]^t \tag{6}$$

$$f = [iu_x, \, iu_y, \, u_z; \, it_{xz}, \, it_{yz}, \, t_{zz}]^t \tag{7}$$

respectively.

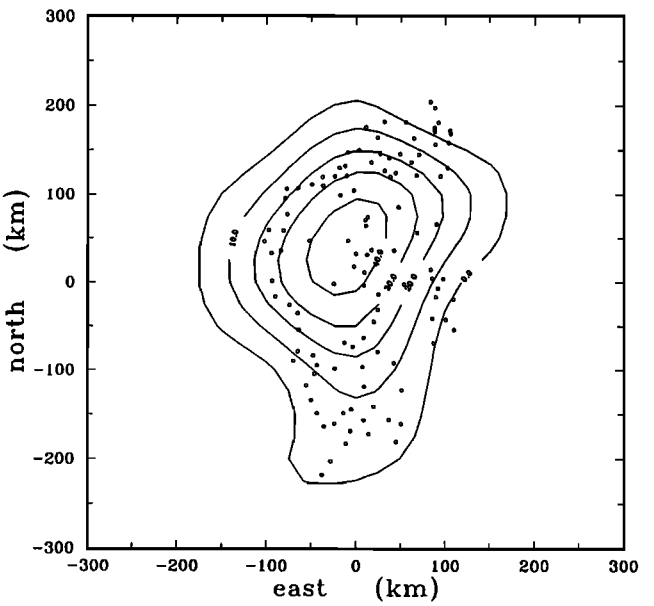

Figure 3a. Observed deflection pattern for Provo epoch. Map View. Contours indicate excess elevation relative to 1453.5 m. The edges of this figure correspond to the large square in Figure 1.

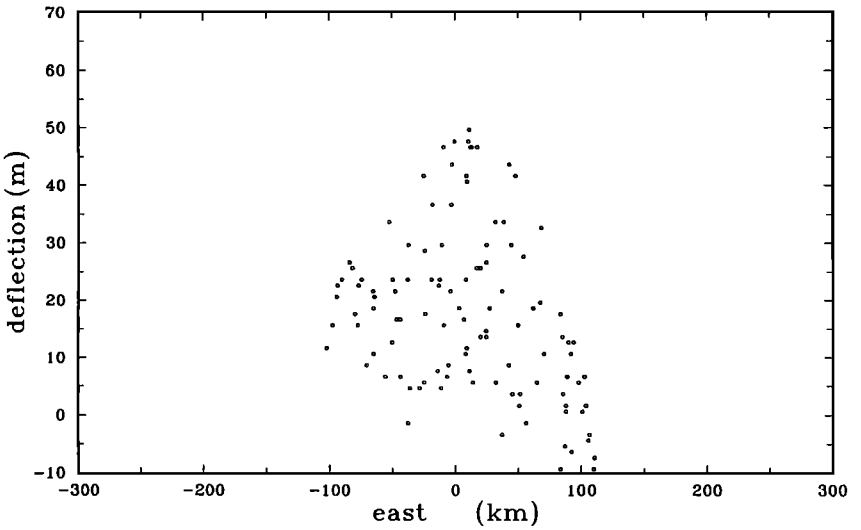

Figure 3b. East-west projection for Provo epoch.

The solution to equations of this type can always be expressed in the form [*Gilbert and Backus*, 1966; *Gantmacher*, 1974]

$$f(k, z) = P(k;\ z + \Delta z, z)\ f(k, z). \tag{8}$$

Multiplication by the propagator matrix P thus transforms a solution at depth z into the corresponding solution at depth $z + \Delta z$.

In outline form, the solution algorithm for an Earth model composed of a uniform half-space substrate, overlain by a number of homogeneous layers, simply consists of selecting downward decaying eigenvectors in the substrate, propagating them to the surface, and then finding a linear combination of them which satisfies the free surface boundary conditions. A suitable pair of solution vectors are

$$\varphi_{-k} = e^{-kz}\ [(1,\ 1);\ -\rho g(2c\hat{k},\ 1 + 2c\hat{k})]^t \tag{9}$$

$$\gamma_{-k} = e^{-kz}\ [(1,\ -c^2);\ -\rho g(2cs^2\hat{k},\ -c^2)]^t \tag{10}$$

where the dimensionless wavenumber $\hat{k}$ is related to the dimensional wavenumber k via

$$\hat{k} = \frac{\alpha\beta k}{g}, \tag{11}$$

and we have defined the dimensionless quantities

$$c = \beta/\alpha \tag{12}$$

$$s^2 = 1 - c^2 \tag{13}$$

in terms of compressional and shear wave speeds in an elastic medium

$$\alpha = \sqrt{(\lambda + 2\mu)/\rho} \tag{14}$$

and

$$\beta = \sqrt{\mu/\rho} \tag{15}$$

respectively.

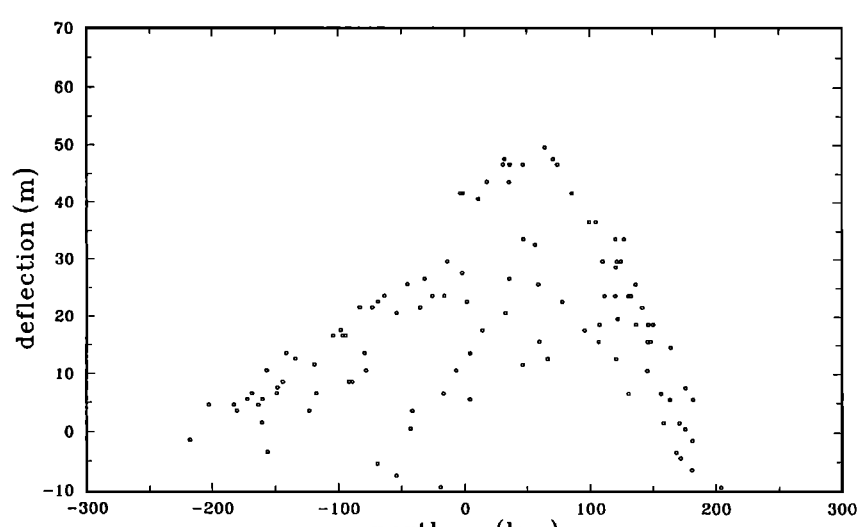

Figure 3c. North-south projection for Provo epoch.

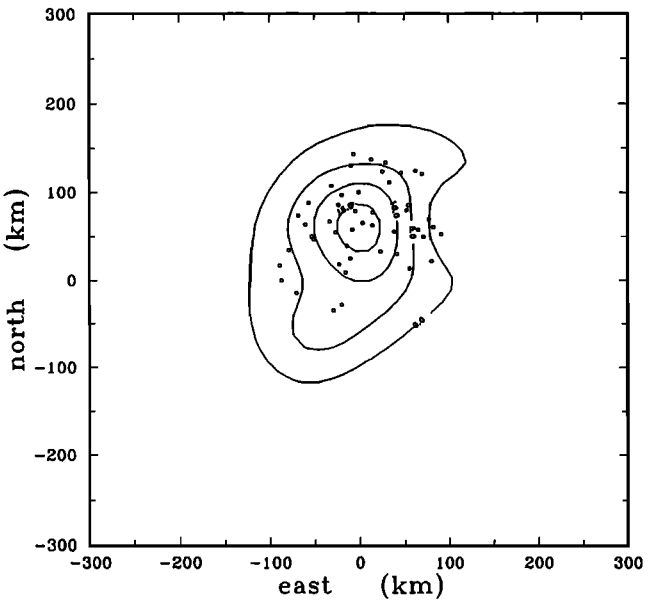

Figure 4a. Observed deflection pattern for Gilbert epoch. Map View. Contours indicate excess elevation relative to 1295.4 m. The edges of this figure correspond to the large square in Figure 1.

The propagator can be written formally as a matrix exponential:

$$P(k;\Delta z) = e^{M(k,z)\Delta z}. \tag{16}$$

The explicit form of the propagator for poloidal displacements in an elastic medium with gravitational effects included via interface forces is given in electronic supplement Appendix C.

The final step in the solution algorithm for an elastic Earth model is to find a linear combination of the two solution vectors

$$h(z) = c_f \varphi_{-k}(z) + c_g \gamma_{-k}(z) \tag{17}$$

which satisfies the appropriate boundary conditions on the stress components t_{rz} and t_{zz}. The weighting factors c_f and c_g, and the surface values of the displacement components $u_r(0)$ and $u_z(0)$ are obtained from

$$\begin{pmatrix} \phi_1 & \gamma_1 & -1 & 0 \\ \phi_2 & \gamma_2 & 0 & -1 \\ \phi_3 & \gamma_3 & 0 & 0 \\ \phi_4 & \gamma_4 & 0 & 0 \end{pmatrix} \begin{pmatrix} c_f \\ c_g \\ u_r(0) \\ u_z(0) \end{pmatrix} = \begin{pmatrix} 0 \\ 0 \\ t_{rz}(0) \\ t_{zz}(0) \end{pmatrix}. \tag{18}$$

The elastic displacements due to applied stresses can now be written in terms of the independent solutions:

$$u_r(z) = \frac{t_{rz}(0) * m(1,4;z) - t_{zz}(0) * m(1,3;z)}{m(3,4;z)} \tag{19}$$

$$u_z(z) = \frac{t_{rz}(0) * m(2,4;z) - t_{zz}(0) * m(2,3;z)}{m(3,4;z)}, \tag{20}$$

where

$$m(i,j;z) = \varphi_i(z) * \gamma_j(z) - \varphi_j(z) * \gamma_i(z) \tag{21}$$

are the minors of the fundamental matrix.

Our primary interest is in the case where the shear stress t_{rz} vanishes at the surface. Appropriate to that case, we define filters which relate surface displacements to applied normal stresses:

$$F_r = u_r(0)/t_{zz}(0) \tag{22}$$

$$F_z = u_z(0)/t_{zz}(0). \tag{23}$$

If the Earth model consists of a uniform half-space, the filters assume particularly simple forms

$$F_r = \frac{-c^2}{\rho g}\left(\frac{1}{1+ak}\right) \tag{24}$$

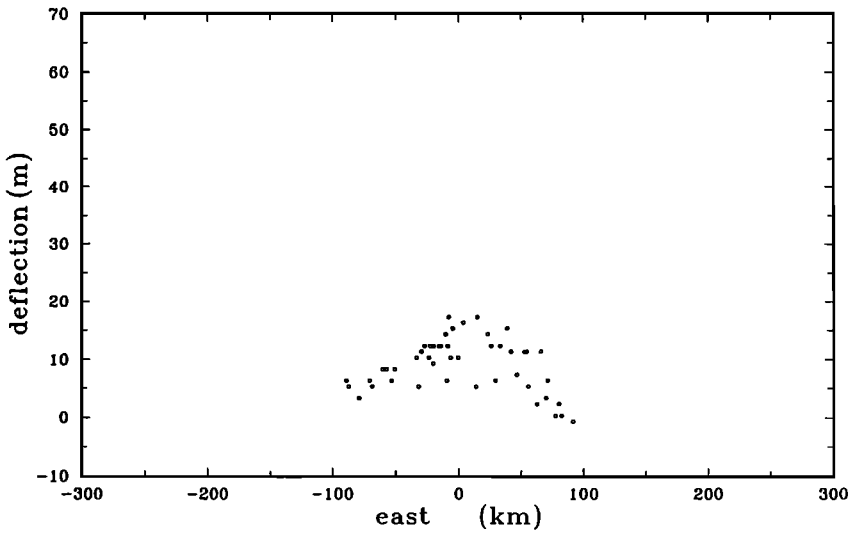

Figure 4b. East-west projection for Gilbert epoch.

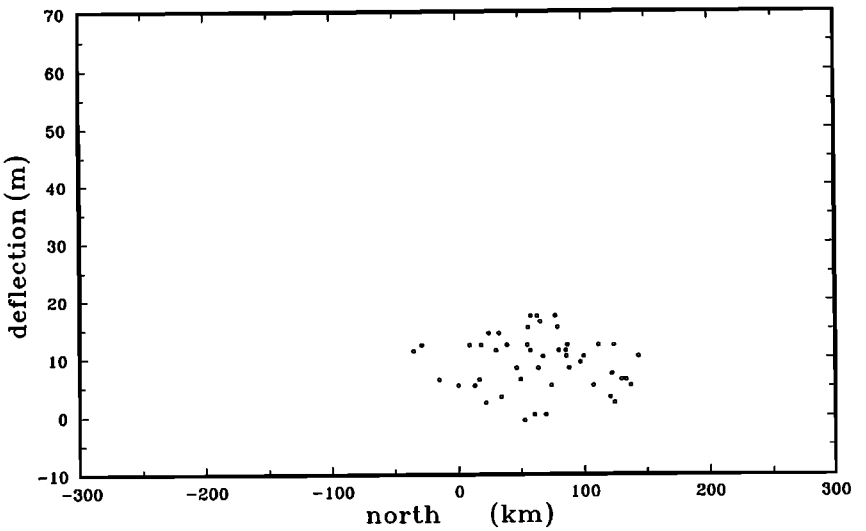

Figure 4c. North-south projection for Gilbert epoch.

$$F_z = \frac{1}{\rho g}\left(\frac{1}{1+ak}\right), \tag{25}$$

where we have defined a length scale

$$a = 2\mu s^2/\rho g \tag{26}$$

which characterizes the transition from buoyant support ($ak << 1$) to elastic support ($ak >> 1$).

In the opposite limit of a thin elastic plate over a fluid half-space, the vertical deflection filter is approximated by [*Wyman*, 1950; *Kerr*, 1964]

$$F_z = \frac{1}{\rho g}\left(\frac{1}{1+(bk)^4}\right), \tag{27}$$

where a flexural length scale b is defined by

$$b^4 = \mu s^2 H^3/3\rho g \tag{28}$$

with H representing the plate thickness. We will see that these two simple end-member models approximate the short-term and long-term responses, respectively, of a layered viscoelastic Earth model with realistic rheological stratification. However, it should be emphasized that in our fit to the data, we used the full analytic formulation.

Viscoelastic Model

Once elastic solutions are available, it is a simple matter to convert them to viscoelastic solutions. The key to this conversion is the observation [*Biot*, 1954; *Lee*, 1955; *Peltier*, 1974] that a Laplace transformation on the time variable maps every quasi-static viscoelastic

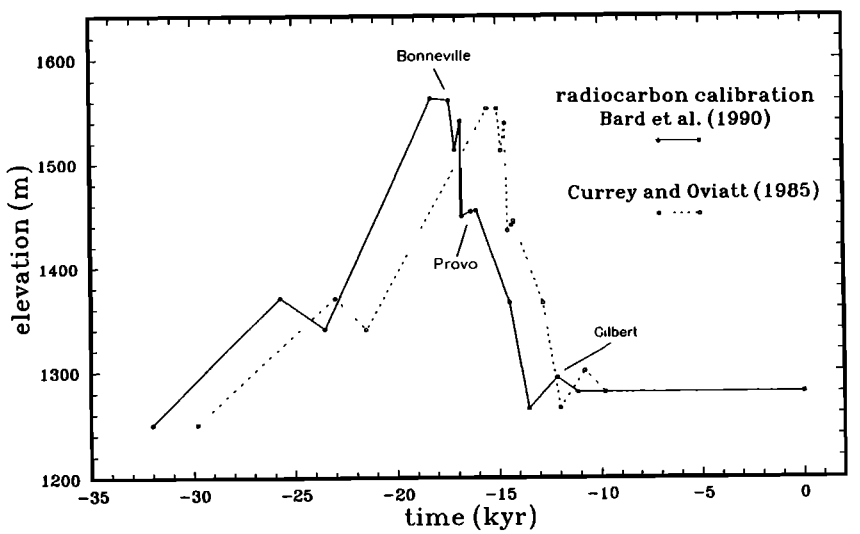

Figure 5. Lake Bonneville elevation history. Dashed lines indicate the lake level model of *Currey and Oviatt* [1985], with ages in radiocarbon years. Solid lines indicate the same chronology with ages converted to calendar years via the calibration of *Bard et al.* [1990] and with elevations of the Bonneville, Provo, and Gilbert epochs adjusted to optimize fit to the shoreline data sets.

problem into an equivalent static elastic problem. In schematic form, the elastic problem consists of determining the displacements $U(x,y)$ due to an imposed normal load $L(x,y)$. The solution is found by the following recipe:

$$\begin{array}{ccc} L(x,y) & \Longrightarrow & \overline{L}(k_x,k_y) \\ & \text{(Fourier)} & \Downarrow \\ U(k,y) & \Longleftarrow & \overline{U}(k_x,k_y) \end{array} \tag{29}$$

The arrow pointing to the right corresponds to a forward transform; the left arrow corresponds to an inverse transform. The downward directed arrow corresponds to multiplication of the transformed load by the appropriate filter. In this same notational scheme, the calculations that yield the viscoelastic response to a time dependant load looks like

$$\begin{array}{ccccc} L(x;t) & \Longrightarrow & \overline{L}(k;t) & \Longrightarrow & \widehat{L}(k;s) \\ & \text{(Fourier)} & & \text{(Laplace)} & \Downarrow \\ U(x;t) & \Longleftarrow & \overline{U}(k;t) & \Longleftarrow & \widehat{U}(k;s) \end{array} \tag{30}$$

where x and k are now taken to be two-vectors.

We assume that the spatial and temporal variations in the load are separable and that the temporal variation is piecewise linear [*Bills and May*, 1987]. The viscoelastic filters are obtained from their elastic counterparts by replacing the elastic moduli with appropriate Laplace transformed compliances.

We follow the standard collocation procedure for the inverse Laplace transformation [*Schapery*, 1961; *Cost*, 1964; *Peltier*, 1974; *Mitrovica and Peltier*, 1992]. We first partition the filter into elastic and viscous parts

$$F(k,s) = F_e(k) + F_v(k,s) \tag{31}$$

where the elastic component is

$$F_e(k) = \lim_{k \to \infty} F(k,s). \tag{32}$$

Next, we solve for a set of coefficients $b_i(k)$ such that

$$F_v(k,s) = \sum \frac{b_i(k)}{(s+s_i)} \tag{33}$$

at the points $s = s_i$. The inverse transform of this collocation function is particularly simple

$$F_v(k,t) = \sum b_i(k)\, e^{-s_i t}. \tag{34}$$

In the actual computations to be presented below, we have used nine Laplace domain samples for each filter inversion. The samples are logarithmically spaced and span the interval

$$10 \text{ years} \leq 1/s_i \leq 10^5 \text{ years}. \tag{35}$$

It is well established that on short time scales the crust and mantle behave as elastic solids, and on very long time scales the mantle behaves as a viscous fluid. How the intermediate time scale behavior relates to either of these end-members is less clear [*Weertman*, 1978]. Also, the relationship of deformation mechanisms on the scale of individual crystals to that on a tectonic scale is still somewhat obscure [*Ashby and Verrall*, 1977; *Smith and Carpenter*, 1987]. In particular, there is considerable interest in knowing whether the deformation associated with glacial and lacustrine loads represents a transient component of the relaxation spectrum, or whether it directly probes the rheology that is relevant to convective flow on much longer time scales [*Peltier*, 1985,1986; *Sabadini et al.*, 1985]. On a regional scale, there is also a problem of relating the rheological stratification inferred, for example, from Lake Bonneville studies [*Nakiboglu and Lambeck*, 1982,1983; *Bills and May*, 1987] to the inferences from Basin and Range tectonics [*Fletcher and Hallet*, 1983; *Smith and Bruhn*, 1984; *Zuber et al.*, 1986; *Bird*, 1988].

For these reasons, we will consider two different rheological models. The classical Maxwell material behaves as an elastic solid on short time scales and as a viscous fluid on long time scales. We also consider a model that has a transient creep response like the Kelvin model, in addition to the steady creep and initial elastic strain of the Maxwell model. The simplest rheological model with these properties is a Burgers body [*Burgers*, 1935; *Gittus*, 1975; *Peltier et al.*, 1981]. Its conventional mechanical analog is a series connection of Kelvin and Maxwell elements. However, *Muller* [1986] has shown that corresponding to any Burgers body, there is a mechanically equivalent model composed of two Maxwell elements in parallel. Formulas for the Laplace transform compliances for these models are given in electronic supplement Appendix B.

In the two-element generalized Maxwell model, the long-term viscosity is always larger than the transient viscosity, and a large disparity between the relaxation rates of the separate elements corresponds to a significant difference between the short-term and long-term responses of the system. See *Peltier et al.* [1981, 1986] for more complete discussions of transient rheology.

In Figure 6 we show vertical and horizontal deflection filters for a simple Earth model consisting of an elastic plate over a Maxwell half-space. The different curves correspond to different times (0, 10, 10^2, 10^3, 10^4, 10^5 years) since emplacement of the load. The initial response of the system to a step function load is similar to the elastic half-space response (equation (25)). The final, relaxed response is very similar to the response of an elastic plate over a buoyant fluid substrate (equation (27)). The effect of a transient creep rheology is illustrated in Figure 7, which shows filters for an Earth model identical to that in Figure 6 except that the rheology of the half-space is a two-element generalized Maxwell body in which the ratio of the relaxation times of the constituent elements is 10. It is evident that differences exist between the responses of the two models but that they are subtle and require good spatial char-

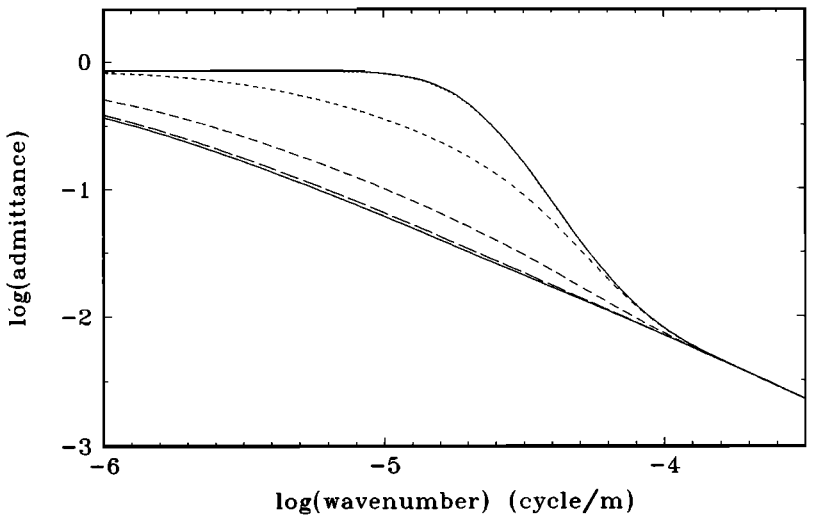

Figure 6a. Vertical deflection filters, elastic plate over Maxwell half-space. The deflections at the surface due to a spatially concentrated unit normal load which is impulsively applied and left in place are computed at times (0, 10, 10^2,10^3,10^4, and 10^5) years after emplacement. Substate viscosity is 10^{20}Pa s. Responses are normalized by the buoyant vertical displacement in a fluid with density equal to the surface density of the Earth model.

acterization of the response at intermediate time scales. The initial and final states are identical.

Another way to introduce multiple relaxation times into the model is to allow the viscosity to vary as a function of depth. Figure 8 illustrates vertical deflection filters for a number of different models. In all cases the top layer is elastic and the substrate is a Maxwell half-space with the same viscosity as in Figure 6. The variation among the cases is due to replacing the bottom 2, 5, or 10 km of the elastic plate with a Maxwell material with viscosity 100 times less viscous than the underlying half-space. In all illustrated cases, the initial response is just that of an elastic half-space. The final response is that of an elastic plate over a fluid substrate. The major difference among the cases illustrated is the mode of transformation from the initial to the final state. It is obvious that as with the transient creep rheology, observations at appropriate wavelengths and time intervals should be able to distinguish between these cases.

Fitting Model to Data

Up to this point, we have described our implementation of the forward modeling procedure. Given an Earth model and a loading history, we can use that formulation to compute the present pattern of deflection that would result on each of several shorelines. We now need an efficient way to convert this forward modeling capability into an inverse modeling capability, so that we can explore the range of Earth model parameters which are consistent with the observational dataset. In the modeling exercise of *Bills and May* [1987], there were only

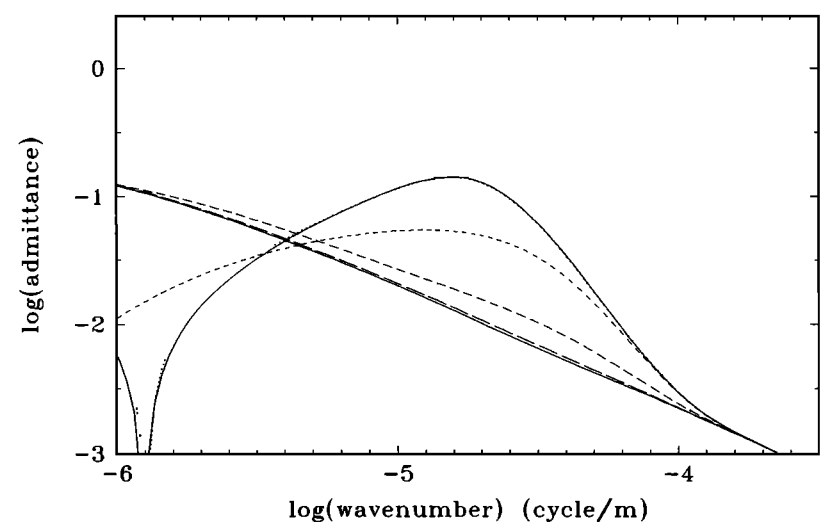

Figure 6b. Same as Figure 6a, except horizontal deflection filters.

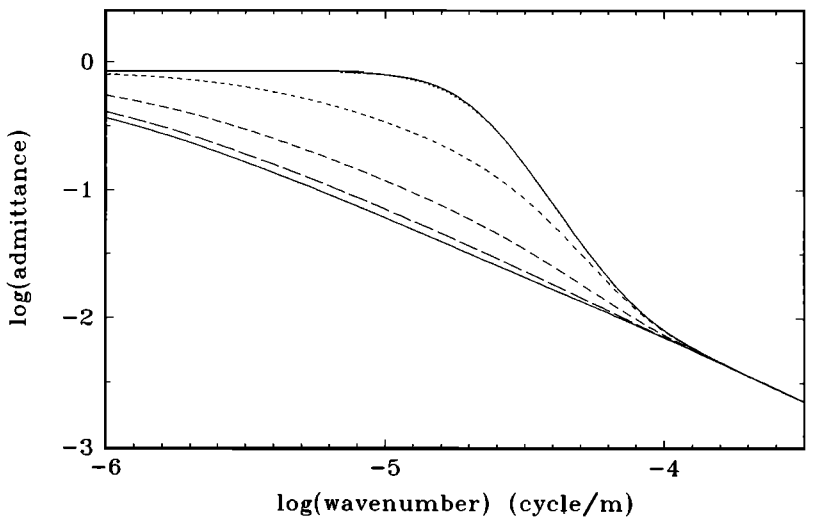

Figure 7a. Vertical deflection filters, elastic plate over generalized Maxwell half-space. Same as Figure 6 except that substrate is two element generalized Maxwell material.

three significant Earth model parameters (elastic lithosphere thickness, upper mantle viscosity, and depth to a rigid substrate). In that case it was feasible (though time consuming) to do a brute force parameter space search. In the present case, we are interested in examining a much higher-dimensional parameter space, and direct exploration of that space, even on a coarse grid, would be prohibitively expensive. Therefore we are obligated to take a different approach.

The approach we have chosen is an iterative, damped least squares estimation procedure. The first step in the procedure is to compute a series of forward models, one with a nominal set of parameter values, and each of the others with a single parameter perturbed from the nominal value. The results of these forward models are then used to numerically compute partial derivatives of the data with respect to each of the parameters. Once the matrix of partial derivatives is computed, it is a simple matter to estimate perturbations to the parameter values which will reduce the residuals. As this is a highly nonlinear problem, we will need to iterate the solution process a number of times. The nature and quality of our final solution will depend on several factors: the quality of the data, the numerical stability of our forward modeling algorithm, and the manner in which we choose to specify the "solve-for" parameters.

We have chosen two different approaches to the parameterization issue. In each case, the elastic parameters (λ, μ, ρ) are held fixed at the values determined by *Priestley et al.* [1980] from seismic travel time data in the Great Basin, and we are using the shoreline deflection data to constrain the viscosity versus depth profile. We also allow the loading history to be adjusted slightly. The epochs of the Bonneville, Provo, and Gilbert shorelines are all given a priori uncertainties of 200 years. The epochs and lake level at those epochs are adjusted to optimize the fit to the deflection data. Relative elevations of the lake at nearby times are kept in proportion.

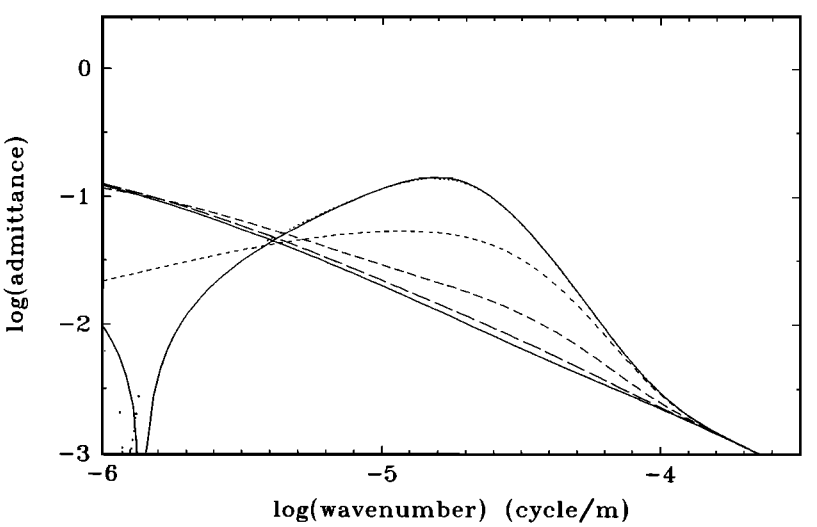

Figure 7b. Same as Figure 7a, except horizontal deflection filters.

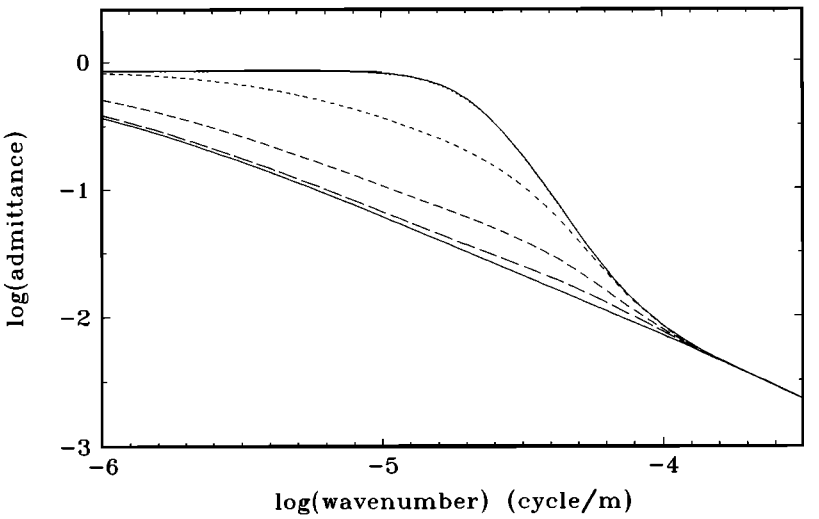

Figure 8a. Deflection filters, elastic plate over weak channel and Maxwell half-space, for 28 km plate and 2 km channel.

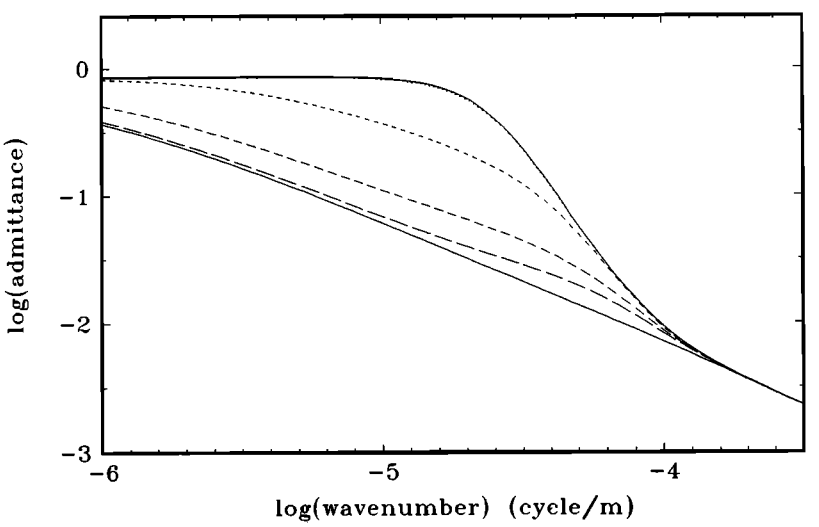

Figure 8b. Same as Figure 8a, except for 25 km plate and 5 km channel.

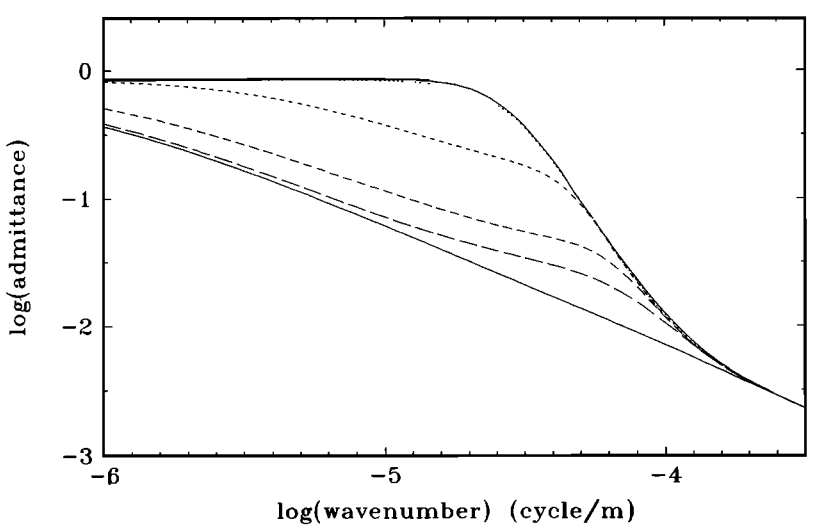

Figure 8c. Same as Figure 8a, except for 20 km plate and 10 km channel.

None of adjustments to the loading history exceeded 300 years or 5 m.

Orthogonal Polynomial Solutions

One approach to specifying independent viscosity values in each of several layers is to enforce some smooth variation of viscosity with depth. A simple way of doing that is to construct a family of orthogonal polynomials to parameterize variations in log(viscosity) versus log(depth). We expect all of the resolvable viscosity variations to take place over some finite depth range, and we desire the variations to transition smoothly to the underlying substrate value. If we take the normalized log(depth) range to run from -1 (at the bottom) to +1 (at the top), an infinite family of orthogonal polynomials is uniquely defined by the three conditions of (1) unit value at the top

$$P_n(x)\,|_{x=1} = 1, \tag{36}$$

(2) zero derivative at the bottom

$$\frac{dP_n(x)}{dx}\,|_{x=-1} = 0, \tag{37}$$

and (3) orthogonality over the interval

$$\int_{-1}^{1} P_n(x)P_m(x)dx = A_n\delta_{nm}. \tag{38}$$

The first few such polynomials have the values

$$P_0(x) = 1 \tag{39}$$

$$8P_1(x) = -1 + 6x + 3x^2 \tag{40}$$

$$8P_2(x) = -3 - 6x + 9x^2 + 8x^3 \tag{41}$$

$$16P_3(x) = 5 - 16x - 36x^2 + 28x^3 + 35x^4 \tag{42}$$

$$16P_4(x) = 3 + 24x - 36x^2 - 92x^3 + 45x^4 + 72x^5 \tag{43}$$

$$128P_5(x) = -37 + 114x + 669x^2 - 612x^3 - 1755x^4 + 594x^5 + 1155x^6 \tag{44}$$

$$128P_6(x) = -15 - 250x + 375x^2 + 2020x^3 - 1265x^4 - 4026x^5 + 1001x^6 + 2288x^7 \tag{45}$$

and are illustrated in Figure 9. The first two polynomials together allow a smooth (quadratic) transition from some surface value of viscosity to the underlying substrate value. As the use of these polynomials enforces smooth variations, we can more readily address the reality of any features that do emerge. The propagator matrix formulation still requires constant material properties in each layer. The polynomial solutions are used to derive a smooth function of depth, and the value of the viscosity in each layer was taken to be the value of the polynomial at the mid-depth of the layer. The usual implementation of this scheme started with a small number of polynomials (2-3) and iterated the solution algorithm until no appreciable further change was noted. Then some additional polynomials were added, and the solution was again iterated to convergence.

A significant feature of this modeling scheme is that, by design, it generates smooth profiles of viscosity versus depth, as would be expected if temperature and pressure were the dominant controls on rheology. However, since compositional variations with depth can yield abrupt changes in viscosity, the results of this approach can possibly be somewhat misleading.

Multiple Independent Layers

An even simpler approach is to merely specify the bounding depths of several viscoelastic layers and to use the observations to estimate the viscosity in each of those layers and in the underlying half-space. If we allowed both the viscosities and bounding depths to vary the problem would be significantly more nonlin-

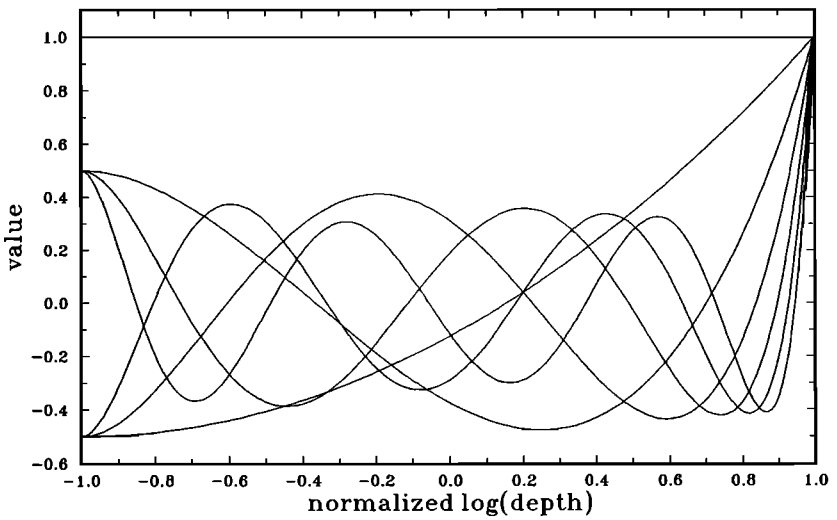

Figure 9. Orthogonal polynomials. This family of orthogonal polynomials is constructed to allow smooth representations of log(viscosity) versus log(depth).

ear. The usual implementation of this scheme started with a small number of layers (4-6) and iterated the solution algorithm until no appreciable further change was noted. Then some, or all of the original layers were subdivided and the solution again iterated to convergence.

An advantage of this approach is its extreme simplicity. A disadvantage is that even with associated formal covariance analyses, it is frequently difficult to assess whether features that emerge are real or spurious.

Results

Elastic Plate and Maxwell Half-Space

The simplest model we considered consists of a single elastic layer overlying a uniform Maxwell half-space. We estimated two parameters: thickness of the elastic plate and viscosity of the half-space. This model is very similar to that employed by *Bills and May* [1987], and the results obtained are very similar. The parameter values which yield the best fit to all of the data are plate thickness of 25 km, half-space viscosity of 1.8×10^{19} Pa s. The residual variance for that solution is 9.7% of the data variance.

Assigning realistic and meaningful uncertainties to these estimates is complicated by the fact that each of the three epochs (Bonneville, Provo, and Gilbert) yields a qualitatively different set of constraints on the parameter values. The Bonneville epoch data are best fit by plate thickness values of 25 $\pm$ 5 km, and any positive viscosity value $\leq 10^{20}$ Pa s is acceptable. The Provo epoch data are best fit by plate thickness values of 27 $\pm$ 5 km, and viscosity values of 10^{19}-10^{20} Pa s are all acceptable, but higher or lower values are strongly excluded. The Gilbert epoch data are rather insensitive to plate thickness but are best fit by viscosity values of 2×10^{20} Pa s, with either higher or lower values excluded. If all the data are given weights proportional to estimates of the associated measurement errors, the Bonneville epoch dominates the overall solution, simply because that epoch has the largest number of measurements. If the plate thickness is held at 25 km, but the viscosity value is increased to 10^{20} Pa s, the overall residual variance increases to 14.2% of the data variance. That solution has over twice the residual variance of the optimal parameters for the Bonneville epoch data but does less damage to the constraints provided by the Provo and Gilbert epochs. This minor discordance among epochs might be indicative of an error in the presumed chronology but is more likely symptomatic of too simple a model.

Generalized Maxwell Half-Space

The next level of complexity in modeling that we considered adds one additional parameter: the elastic plate is unchanged, but the Maxwell half-space is allowed two viscosities, enabling separate transient and steady state relaxation times. We examined models with elastic plate thicknesses in the interval 15-35 km and for which the two elastic elements of the generalized Maxwell material were equal. The viscous elements were constrained to the range 10^{18}-10^{21} Pa s. For both the Bonneville and Provo epoch data, solutions were found which fit the data marginally better than any corresponding single Maxwell element model. The best fit to the Bonneville epoch data alone had a plate thickness of 25 km, and viscosities of 10^{18} and 3×10^{19} Pa s. For that model, the total residual variance (including all three epochs) was 9.4% of the data variance. However, for the Gilbert epoch data, we found that independent of the choice of elastic plate thickness, the best fitting values for the two viscous elements were always equal. In that case the generalized Maxwell model reduces to a classic, single-element model. The model values which best fit all of the data (Bonneville, Provo and Gilbert epochs) are identical to the two-parameter model discussed in the preceding paragraph. We conclude that over the range of parameter values we explored, there is no compelling evidence for a rheology more complex that the classical Maxwell model. We note that a similar conclusion was reached by *Peltier et al.* [1986] using a global data set of relative sea level curves.

Orthogonal Polynomial Profile

An alternative way of providing for multiple relaxation time scales is to allow the viscosity to vary with depth. In each layer, the rheology was assumed to be classical Maxwell viscoelastic, and the elastic parameters (λ, μ, ρ) were held fixed at the values determined by *Priestley et al.* [1980]. Those values are shown in Figure 10. The rebound data were used to estimate coefficients of a set of polynomials which govern the viscosity profile. The best fitting orthogonal polynomial model we have found in our current search has a constant viscosity of 4×10^{19} Pa s below a depth of 300 km. The coefficients of polynomials beyond the first two are not significantly different from zero. Thus the resulting profile, which is shown in Figure 11, is completely monotonic. Though the model nominally had 7 degrees of freedom (six polynomial amplitudes and an underlying half-space viscosity), only 3 of those degrees of freedom were significantly utilized. The residual variance of this model is 8.7% of the data variance.

The half-space viscosity value is close to previous estimates from the Bonneville data but is rather lower than global scale glacial rebound estimates. It is not yet known whether this disagreement is real and reflects the peculiar properties of the upper mantle beneath the Great Basin or simply results from differences in modeling strategies and input data.

Multiple Independent Layers

In this model, each layer of the Earth model is considered to be a classical, single-element Maxwell material, and the viscosity of each layer is independently esti-

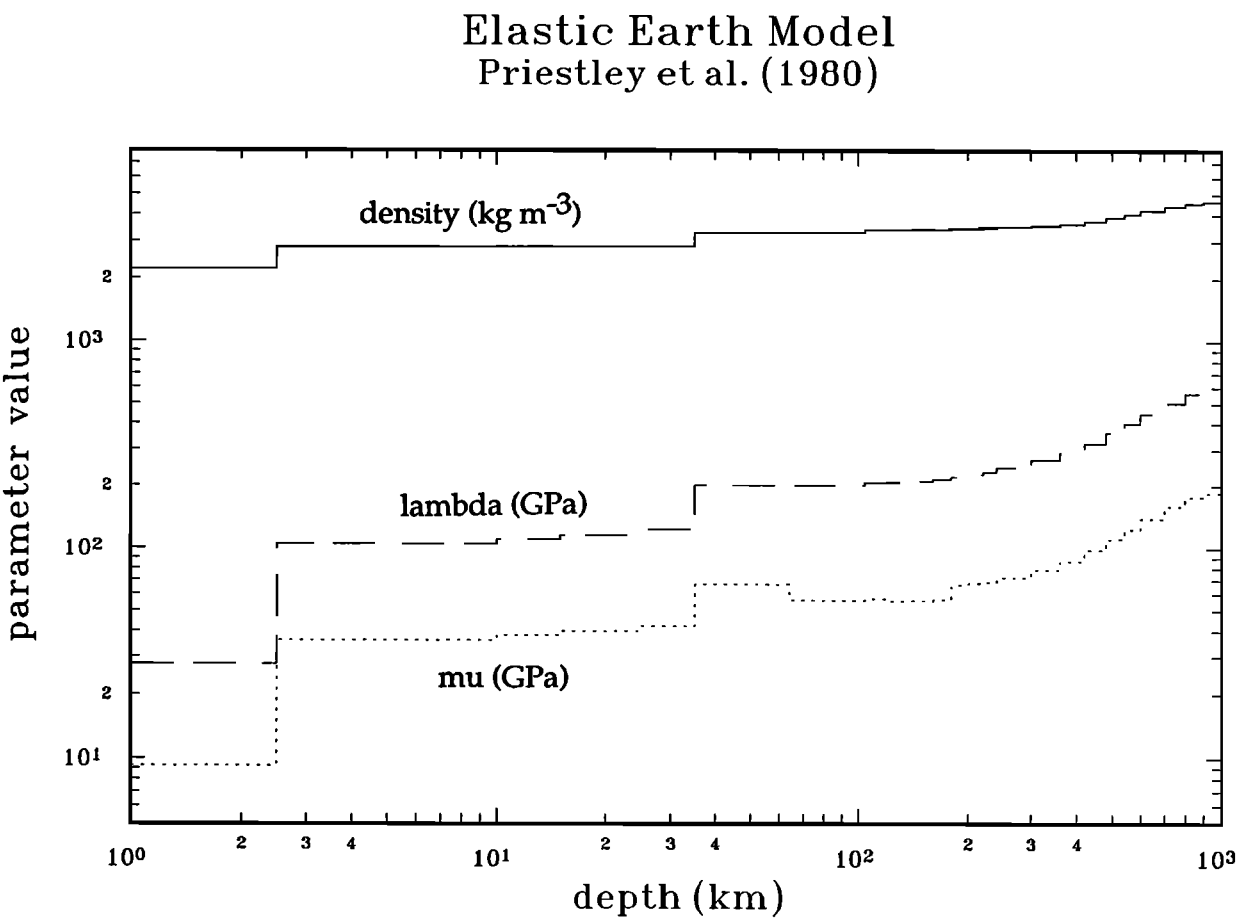

Figure 10. Elastic parameters. These elastic model parameter values were held fixed while viscosity values were estimated from deflection observations.

mated from the rebound data. The best model of this sort that we found in our linearized least squares search contains 10 independent layers. Thus the model effectively had 11 degrees of freedom (10 layer viscosities and an underlying substrate viscosity). The starting point for the damped least-squares solution algorithm had a high viscosity (2×10^{24} Pa s) in the top 20 km, and a lower viscosity (10^{20} Pa s) everywhere below that layer. The resulting profile of viscosity versus depth is shown in Figure 12. A surprising amount of structure emerges in this model. The viscosity drops rapidly from high surficial values to low subcrustal values (10^{18} Pa s from 40-80 km), then rises to a high level in the uppermost mantle (3×10^{20} Pa s from 150-300 km), and then returns to quite low values at mid-upper mantle levels (10^{19} Pa s at 300 km and below).

Figure 13 indicates the depth range over which the Great Basin shoreline data set has significant resolution. The prior standard deviation for the log(viscosity) profile was taken to be 1.0 throughout (upper solid line). It is well known that estimation problems of this sort involve a trade-off between resolution and variance (see *Mitrovica and Peltier* [1991] for a discussion in the context of mantle viscosity). For this analysis, we have chosen layer thicknesses in such a way that they represent uniform steps in log(depth). In this particular case, each layer is thicker than the one immediately above it by the factor $10^{1/5} = 1.585$. The dotted line in Figure 13 represents the posterior standard deviations for a solution using Lake Bonneville shorelines only. The dashed line represents the complete data set (Bonneville, Waring, Clover, and Franklin). Note that with this choice of resolution bins, both solutions have reasonable variance reduction over a depth range from 4 to 250 km, with the best results in the range from 6 to 60 km. Also note that the full solution has its most significant improvement over the Bonneville-only case in two separate depth ranges: 6-15 km and 100-250 km. The former is comparable to the intersite separation distance in the western lake data sets, and the latter is comparable to the scale of the loading.

The computed deflection patterns for this multiple independent layer model at Bonneville, Provo, and Gilbert epochs are illustrated in Figures 14, 15, and 16. The difference between observed and computed values are illustrated in Figure 17. The residual variance of this model is 8.4% of the data variance. Though by some standards this is a good fit to empirical field data, the residuals are much larger that the measurement errors (1-3 m in the Bonneville basin, 0.3-0.6 m in the other

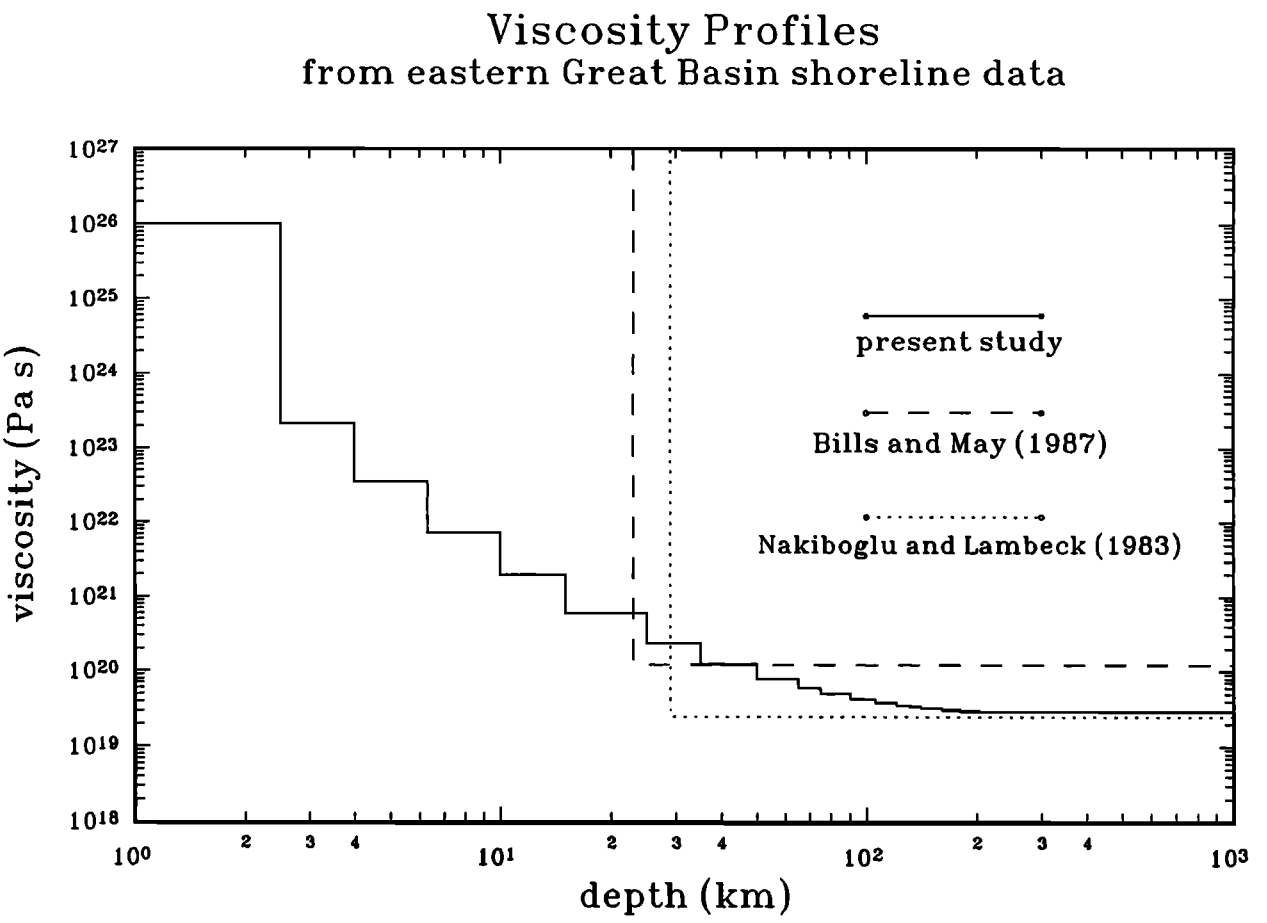

Figure 11. Viscosity profile: orthogonal polynomials. Bounding depths of the layers were arbitrarily selected, and log(viscosity) versus log(depth) profile was estimated using the orthogonal polynomials shown in Figure 9 by minimizing the misfit between calculated and observed values of the spatio-temporal deflection field.

basins). A question also arises concerning the reality of some of the features seen in this model.

The sources of some of the residual elevations are well understood. Some are due to the unmodeled deltaic loads associated with the major tributary rivers (Bear, Weber, and Provo). Others are associated with post-eruptive volcanic collapse, such as occurred at Pavant Butte [*Condie and Barsky*, 1972; *Oviatt and Nash*, 1989], or shallow intrusive uplift, as occurred at Cove Creek Dome [*Condie and Barsky*, 1972; *Oviatt*, 1991]. However, it is quite likely that much of the remainder reflects tectonic motions on individual tectonic blocks within the Basin and Range province. A significantly higher density of measurements throughout the Bonneville basin should reveal such tectonic tilt domains.

As a partial test of the robustness of the modeling results, similar models with different numbers of layers, and different bounding depths for the layers, were also fit to the data. Somewhat surprisingly, a similar pattern emerged in each case for which the test was performed. Some aspect of the rebound data (or possibly some poorly understood quirk in the modeling algorithm) seems to predispose the model to a nonmonotonic viscosity profile, with a low-viscosity channel extending from 40 to150 km, a high-viscosity lid from 200 to 300 km, and a transition to a somewhat lower substrate value. This is not unlike the structure seen by *Beghoul et al.* [1993] in P wave velocity variations in the Basin and Range province.

Discussion

Other Estimates of Western U.S. Structure

Several independent techniques have been used in the past to estimate thickness of the elastic lithosphere in the Basin and Range province. Deformation of the crust accompanying slip on normal faults is consistent with an effective elastic thickness of 2 km or less [*Buck*, 1988; *Stein et al.*, 1988]. The coherence between topography and Bouguer gravity anomalies changes at a wavelength that suggests that the lithosphere responds as an elastic plate with effective thickness of 4-5 km [*Bechtel et al.*, 1990]. Earthquakes occur to a depth of 12-15 km [*Smith and Bruhn*, 1984], which is presumably an indicator of the depth of the transition from elastic-brittle to ductile-viscous behavior [*Sibson*, 1982; *Chen and Mol-*

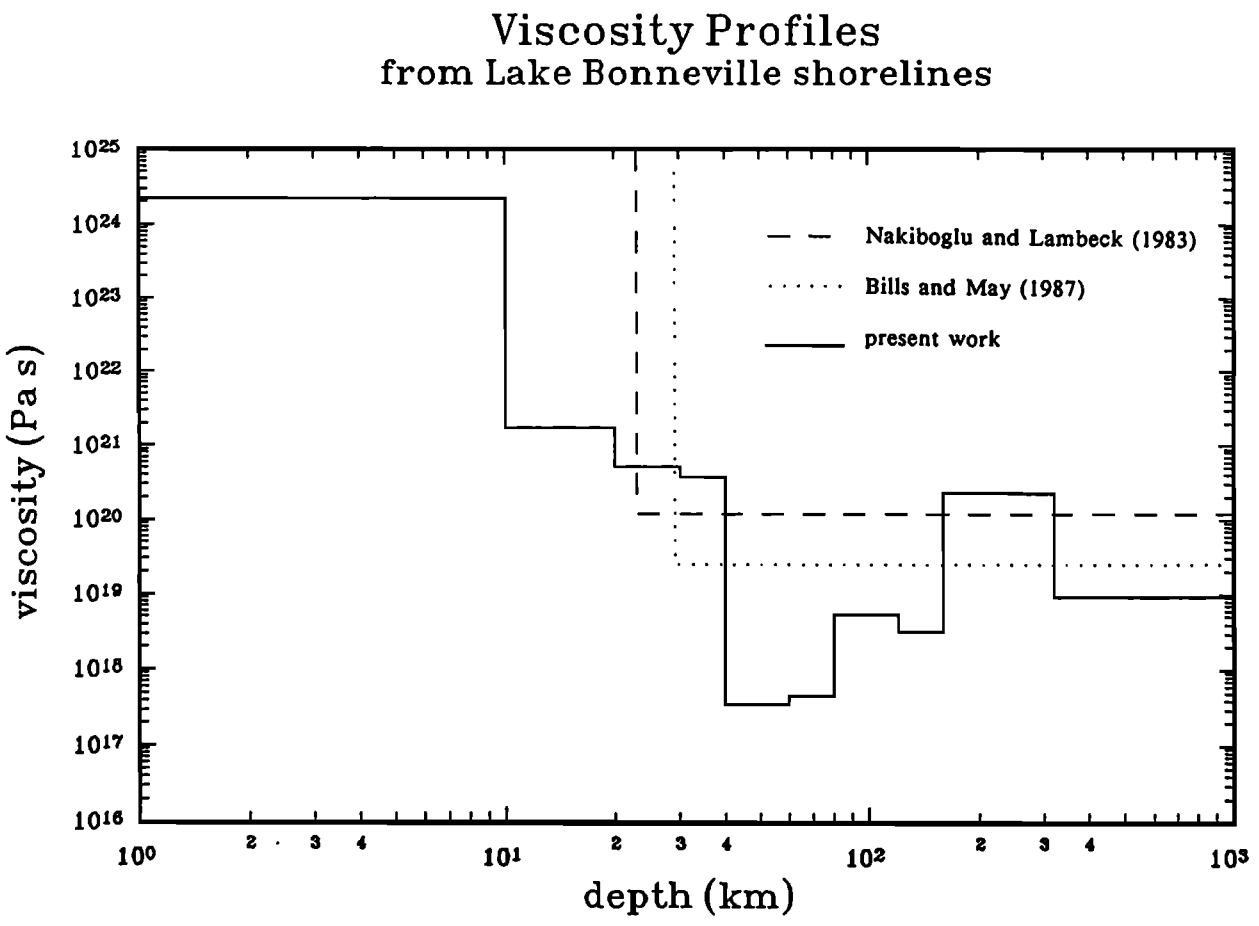

Figure 12. Viscosity profile: independent layer model. Similar to Figure 11, except that viscosity in each layer was independently varied in the estimation scheme.

nar, 1983]. The tectonic structure of the Basin and Range province has two characteristic wavelengths: the typical spacing between ranges is ~30 km, and the typical spacing of tilt domains (regions within which fault blocks dip away from antiformal and toward synformal axes) is ~200 km [*Stewart*, 1980; *Zoback et al.*,,1981]. A model which duplicates this bimodal pattern invokes extensional instabilities in an Earth model with strong upper crust, weak lower crust, and strong upper mantle [*Fletcher and Hallet*, 1983; *Froidevaux*, 1986; *Zuber et al.*, 1986]. The observed domain sizes imply a strong crustal layer ~10 km thick and a mantle layer thickness of 8-18 km. Previous attempts to infer crustal and mantle rheology from patterns of Lake Bonneville shoreline deflection have been reasonably consistent in estimating an elastic plate thickness of 25-40 km [*Crittenden*, 1963a,b; *Nakiboglu and Lambeck*, 1982,1983; *Bills and May*, 1987]. The divergence of results from these various means of estimating lithospheric thickness has contributions from two sources: each of the techniques is actually measuring a slightly different property of the Earth, and all of the models are either underparameterized or are otherwise overly simplistic. A further complication is related to the fact that the upper mantle structure of the western United States is laterally heterogeneous [*Humphreys and Dueker*, 1994a,b].

In the case of the shoreline deflection modeling, the simplest useful model has two parameters: thickness of an elastic plate and viscosity of a Maxwell half-space. From the point of view of reproducing the data, the model is an outstanding success. However, from a conceptual perspective, it is very unsatisfying to have the viscosity take on only two values: infinite in the plate, and a large but finite value in the half-space. A much more reasonable answer is to have the viscosity decrease gradually with depth. In that case, the "effective thickness" of the lithosphere will be dependent on the duration of the load. For lake loads, with characteristic times of 10^2-10^4 years, the "elastic" plate will be the 20-30 km thick region whose relaxation time is long compared with the loading time. For structures built by faulting and sediment infilling over characteristic times of 10^5-10^7 years, the "elastic" plate will only be the top 2-4 km in which the relaxation time is correspondingly long.

Weak Midcrustal Layer

The observation that the Moho is essentially flat throughout the Basin and Range province, despite sig-

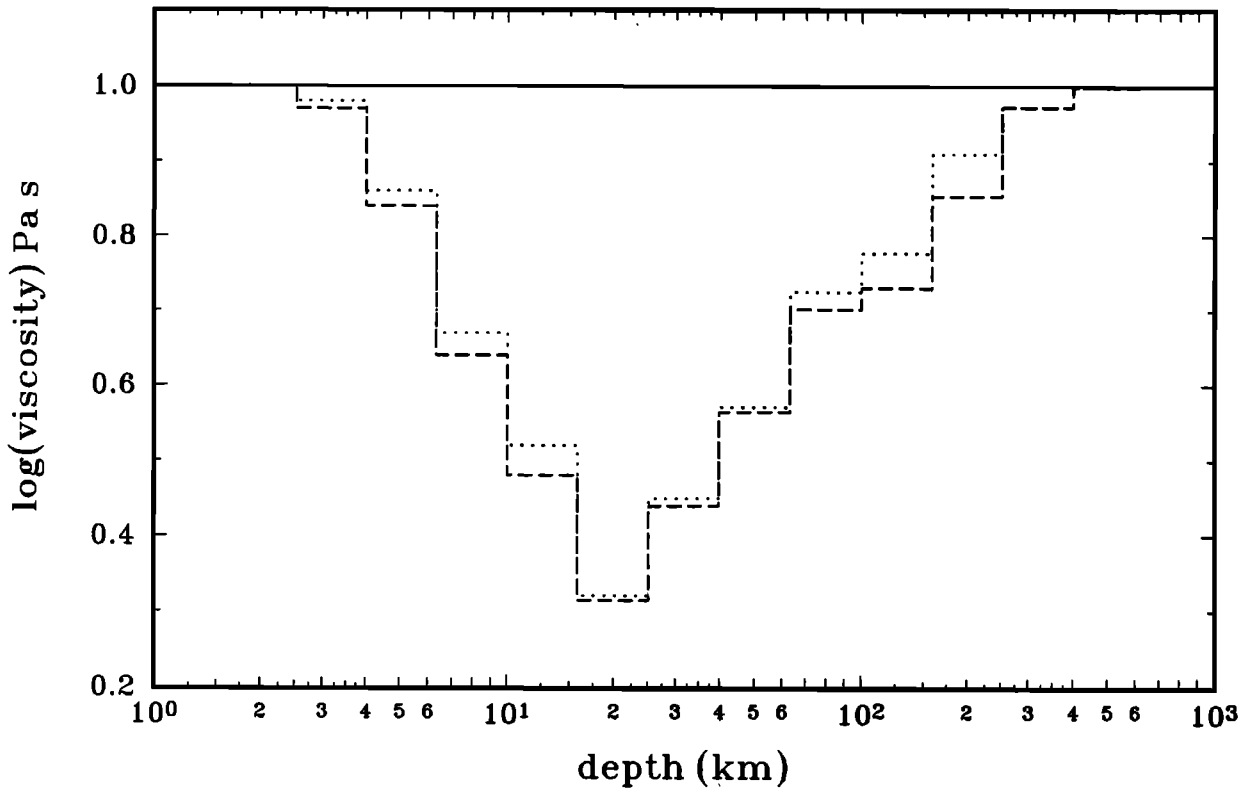

Figure 13. Viscosity error profile: independent layers. Solid line represents prior standard deviations of log(viscosity). Dotted line represents posterior standard deviations for solution using Bonneville data only. Dashed line represents solution using complete data set, consisting of shorelines from lakes Bonneville, Waring, Clover, and Franklin.

nificant relief at the surface, has been interpreted to result from an extremely low viscosity layer at midcrustal depths [*Wernicke and Axen*, 1988; *Kruse et al.*, 1991]. If such a structure does actually exist in the crust, it is reasonable to assume that the rebound data would reveal it [*Ranalli and Murphy*, 1987]. In fact, there are diagnostic differences in the spatio-temporal patterns of surface deflection excited by a point load in the case of flow in a thin low-viscosity channel, versus flow in a uniform half-space. However, we have found in our inverse modeling efforts that the present data set is quite insensitive to the presence or absence of a thin, midcrustal low-viscosity layer. None of our unconstrained models had a mid-crustal low viscosity channel. Furthermore, if we arbitrarily inserted such a layer in our model, it did not significantly influence the inferred underlying structure, unless the thickness and viscosity contrast were both made implausibly large. While we cannot exclude the presence of an unresolved low-viscosity channel, we can confidently exclude the undetected presence of such a feature as the explanation of why the inferred upper mantle viscosity in this region is lower than the global average (as inferred from glacial rebound studies).

Global Estimates of Mantle Viscosity

The upper mantle viscosity estimates obtained in this study, and most previous studies of the Lake Bon-

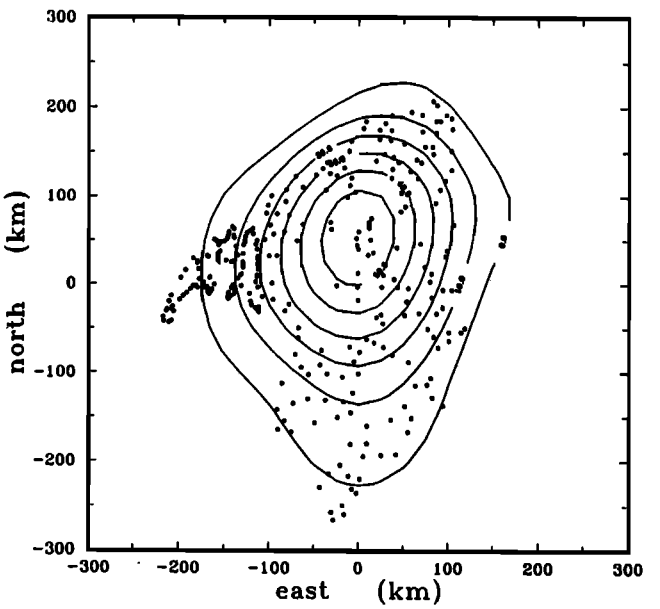

Figure 14a. Computed deflection pattern for Bonneville epoch. Map view. The model shown in Figure 12 was used to calculate the vertical deflection at each location for which an observation was available. Compare to Figure 2. The edges of this figure correspond to the large square in Figure 1.

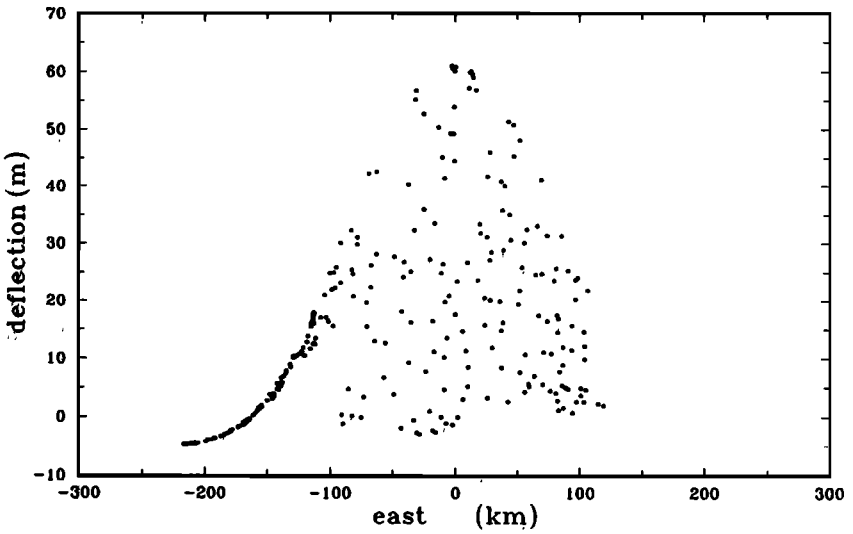

Figure 14b. East-west projection.

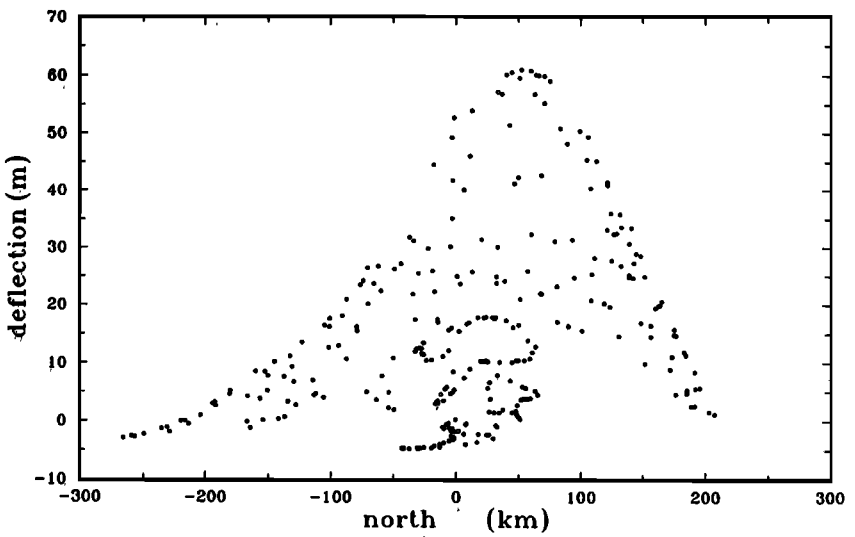

Figure 14c. North-south projection.

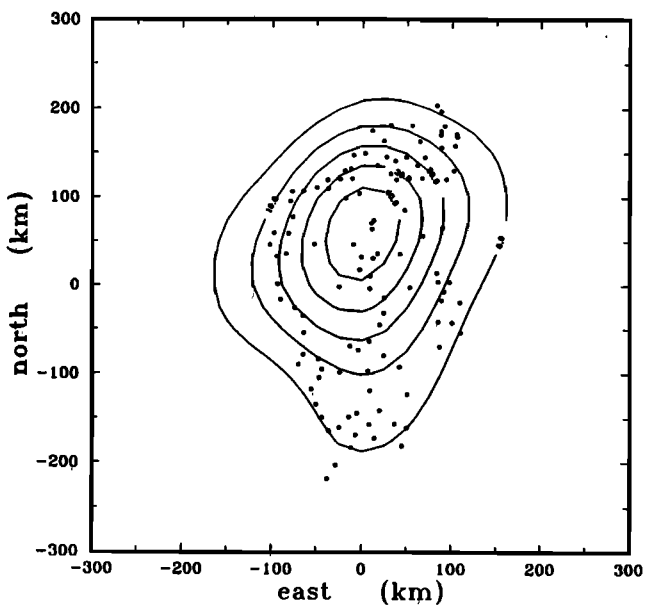

neville shorelines, are 1-2 orders of magnitude lower than the global average upper mantle viscosity estimates obtained from glacial rebound studies [*Peltier et al.*, 1981; *Peltier*, 1986; *Mitrovica and Peltier*, 1991]. One possible explanation for this anomaly is suggested by observations of high heat flow [*Lachenbruch*, 1978], recent volcanism [*Condie and Barsky*, 1972; *Oviatt and Nash*, 1989], and extensional tectonics [*McKee and Noble*, 1986; *Minster and Jordan*, 1987; *Zoback*, 1989]. The essence of this canonical explanation is that the upper mantle has a low viscosity because it is anomalously warm. Though this is a plausible explanation, it is not the only possibility.

Figure 15a. Computed deflection pattern for Provo epoch. Map view. Same as Figure 14, but for Provo shoreline. Compare to Figure 3. The edges of this figure correspond to the large square in Figure 1.

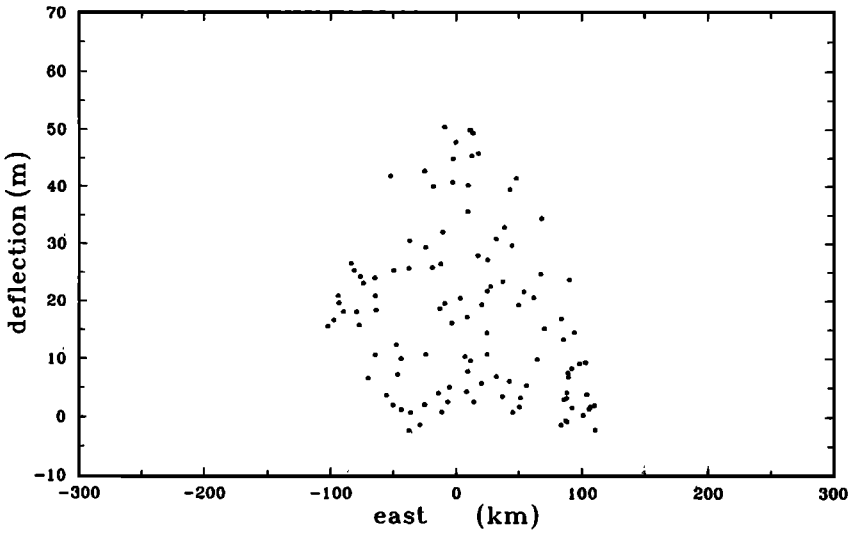

Figure 15b. East-west projection.

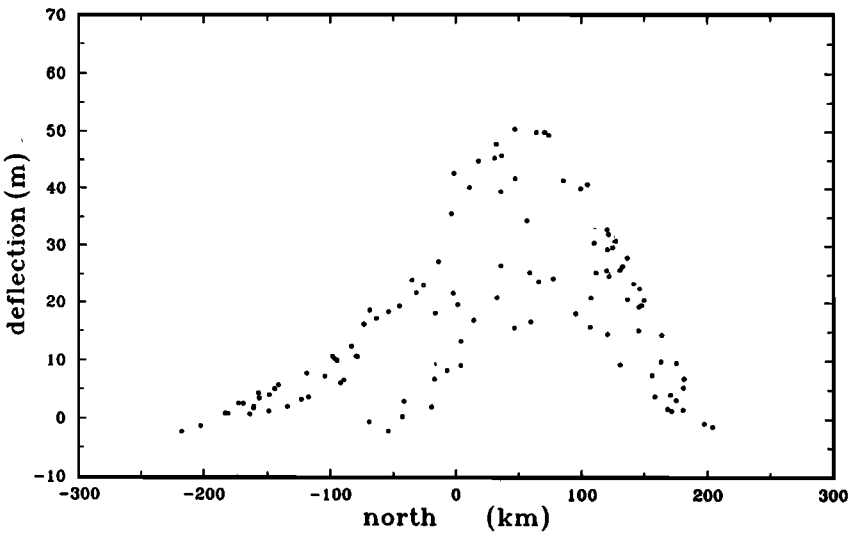

Figure 15c. North-south projection.

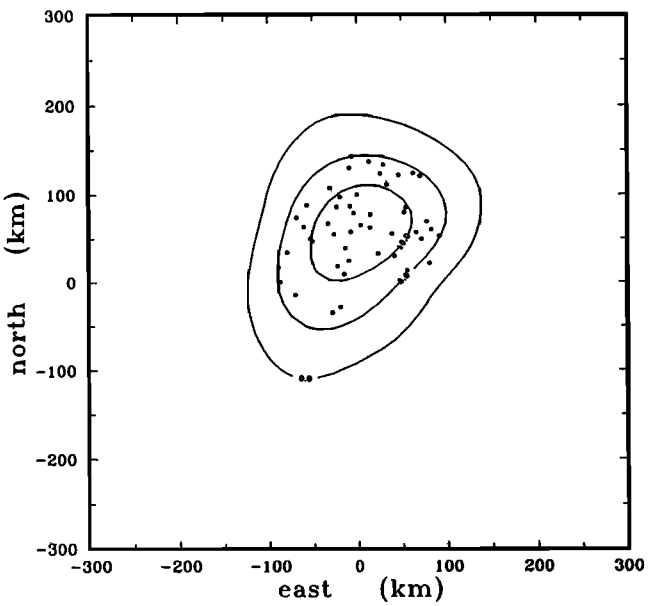

One alternative is that the composition, rather than the temperature, of the Eastern Great Basin upper mantle is anomalous. Relatively minor variations in composition can dramatically influence the solidus temperature of likely mantle mineral assemblages [*Hummel and Arndt*, 1985; *Borch and Green*, 1987]. As high-temperature creep in many materials is strongly dependent on homologous temperature (ambient temperature normalized by solidus temperature), this mechanism is almost certainly operative at some level.

A second alternative invokes variations in ambient tectonic stress. If the relationship between stress and strain rate is nonlinear, as is quite likely the case [*Kirby*,

Figure 16a. Computed deflection pattern for Gilbert epoch. Map view. Same as Figures 14 and 15, but for Gilbert shoreline. Compare to Figure 4. The edges of this figure correspond to the large square in Figure 1.

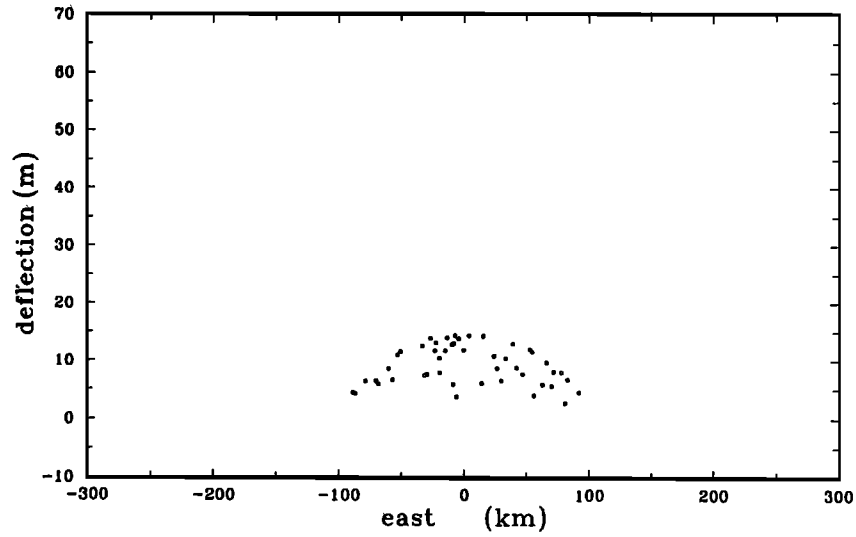

Figure 16b. East-west projection.

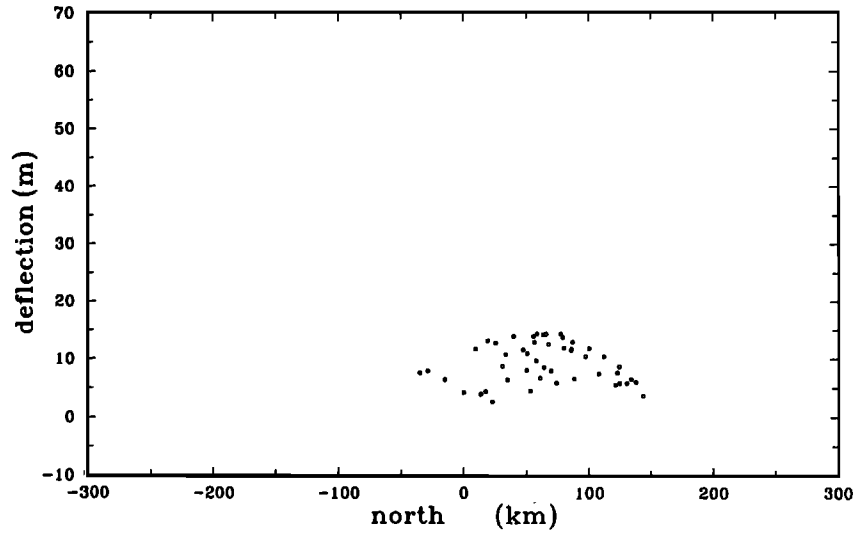

Figure 16c. North-south projection.

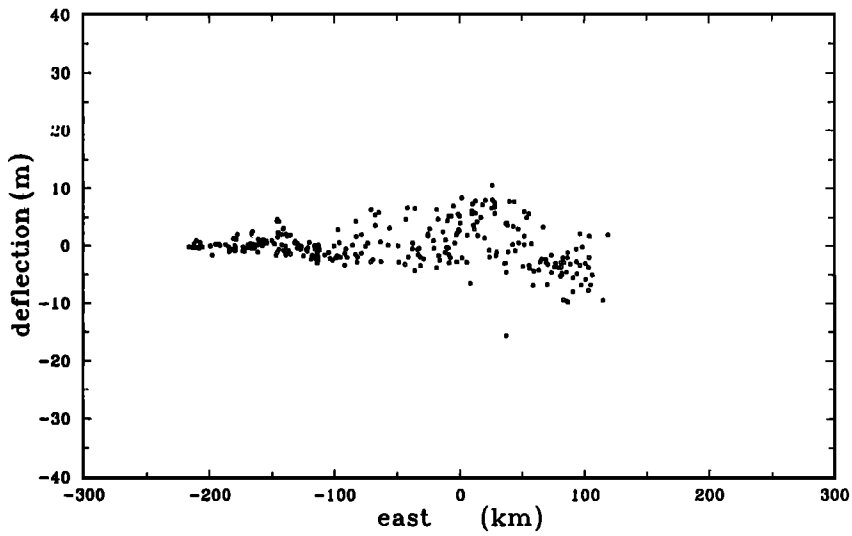

Figure 17a. Residual deflection pattern for Bonneville epoch. East-west projection.

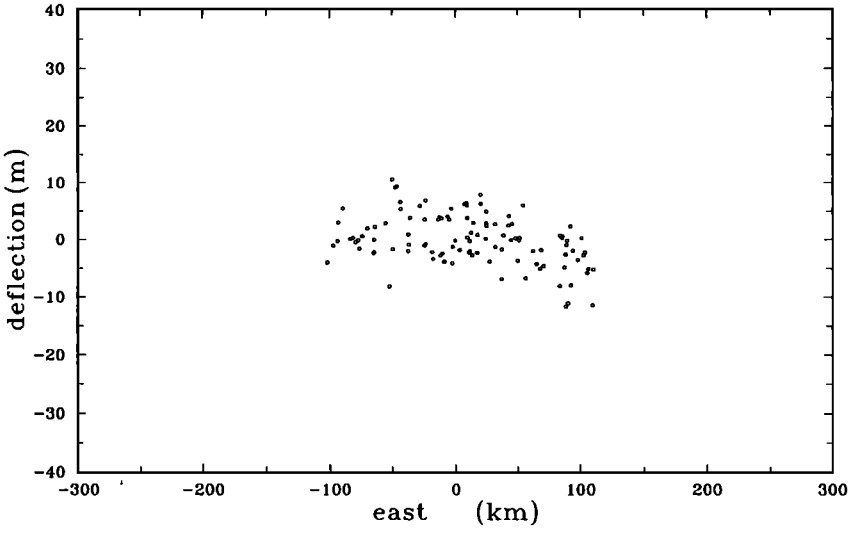

Figure 17b. Same as Figure 17a, exept for Provo epoch.

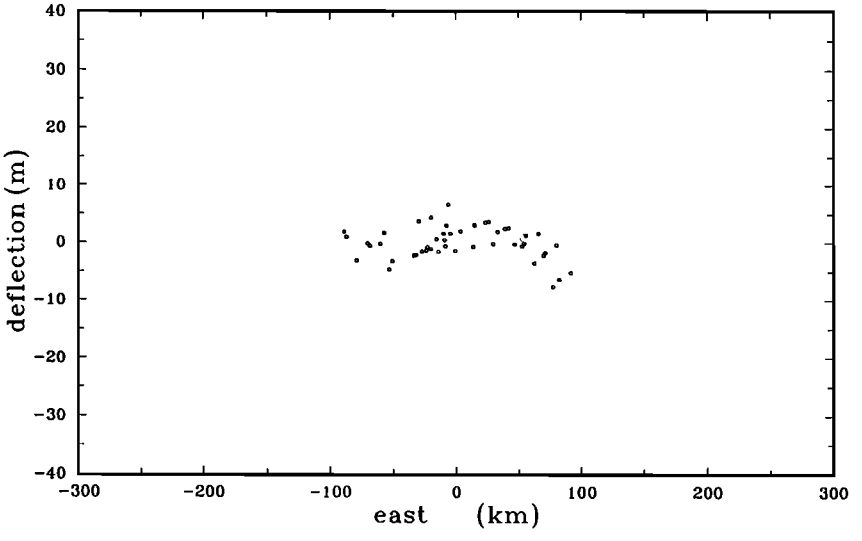

Figure 17c. Same as Figure 17a, except for Gilbert epoch.

1983; *Ranalli and Murphy*, 1987], the effective viscosity seen in response to normal loading will depend on preexisting tectonic stresses [*Brennen*, 1974; *Crough*, 1977; *Weijermars and Schmeling*, 1986; *Kornig and Muller*, 1989]. Regions, such as the Great Basin, that are subjected to relatively high levels of tectonic stress will exhibit lower values of effective viscosity in response to surficial loading than would be seen in lower stress regions under otherwise similar conditions of temperature and composition.

From this perspective, it would be very informative to find another locality in which significant lacustrine loading has occurred but in a very different tectonic setting. Fortunately, such a situation does exist on the Bolivian altiplano. Paleolake Minchin [*Servant and Fontes*, 1978] had a maximum areal extent of ~50,000 km^2, which is virtually identical to Lake Bonneville but was only ~150 m deep. Thus, all else being equal, the highest shorelines should show about 40% as much deflection, or roughly 30 m. A preliminary investigation of the limneotectonics of that basin is currently under way [*Bills et al.*, 1994]. The expectation is that constraints on the effective rheology of the crust and upper mantle will be obtained from the response to the lake load. Comparison of those results, obtained in a region with thick crust, high heat flow, compressive stress regime, and active subduction-driven tectonics [*Barazangi and Isacks*, 1976; *Froidevaux and Isacks*, 1984; *Jordan and Alonso*, 1987; *Isacks*, 1988; *Kono et al.*, 1989] with the Great Basin results reported here, should help resolve some of the ambiguity in interpretation.

Lateral Deflections and Paleoseismicity

Though the observed patterns of paleoseismicity on the Wasatch fault were not used as constraints in any

of the inverse modeling efforts, it is still interesting to present the results of forward modeling of the lateral displacements caused by the Lake Bonneville load. Figure 18 illustrates a representative case. Lateral displacements, computed for a simple two-parameter model (elastic plate thickness of 25 km, Maxwell half-space viscosity of 10^{20} Pa s) at the time of maximum Bonneville epoch loading, are shown as arrows. The trace of the Wasatch fault is also shown. An interesting pattern is beginning to emerge from recent work on the history of interaction between fluctuations in the level of Lake Bonneville and levels of seismicity on the various segments of the Wasatch fault [*Forman et al.*, 1991; *Machette et al.*, 1991]. It had previously been demonstrated by *Schwartz and Coppersmith* [1984] that individual segments of the fault tend to slip independently and that each segment has a characteristic magnitude and frequency of events. The recent work suggests further that on some segments of the fault, the characteristic seismicity was suppressed for most of the last deep lake cycle, and there was a compensating increase in seismicity after the lake fell below the Provo level. Suppression of seismicity on those segments of the fault which are essentially perpendicular to the computed dis-

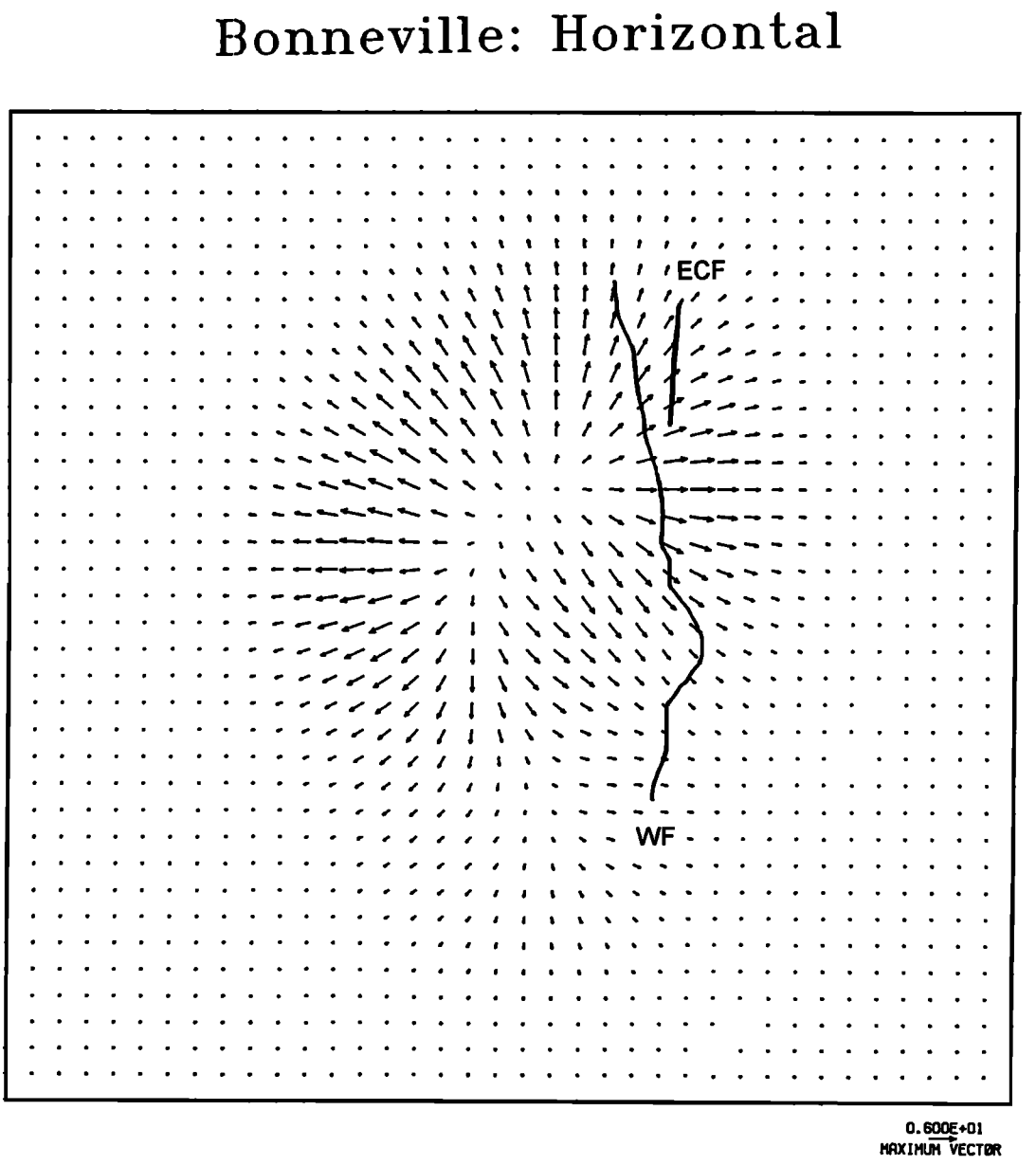

Figure 18. Lateral displacements at Bonneville Epoch. Displacements due to maximum Bonneville load are calculated for a representative simple model with 25 km elastic plate and 10^{20}Pa s viscosity. Note that along several segments of the Wasatch Fault (WF) and the adjacent East Cache Fault (ECF), lake induced displacements are roughly normal to the fault strike. Seismicity along those segments appears to have been diminished during the last deep lake cycle. The edges of this figure correspond to the large square in Figure 1.

placements is compatible with observed patterns [*Forman et al.*, 1991; *Machette et al.*, 1991] and may be explained by two observations. Lateral compressive stress would act to bind the foot wall and hanging wall blocks together, so that normal slip on the fault would be more difficult than usual. An even more important consideration is that the lateral displacement (amounting to 12 m across the width of the basin), would largely counteract the tectonic extension of 5-10 mm/y [*Minster and Jordan*, 1987; *Zoback*, 1989; *Ward*, 1990; *Argus and Gordon*, 1991] which is the ultimate cause of the faulting. In this scenario, seismicity would be reduced or eliminated during deep lake phases and would then subsequently increase to (or even above) the background level upon removal of the lake load.

Rapid historic variations in the level of Great Salt Lake, from a low of 1277.5 m in 1963 to a high of 1283.7 m in 1987, might produce observable lateral displacements [*Savage et al.*, 1985], especially if there were a mid-crustal weak zone, as advocated by *McAdoo and Zilkowski* [1986]. However, recent analysis of measurements taken from 1972 to 1990 on a trilateration network located on the east margin of the lake does not support that notion [*Savage et al.*, 1992].

Acknowledgments. Numerous people have made contributions to this project, both in acquiring the data and in modeling it. Glen May, Stephan Mojzsis, and Susan Sakimoto helped in early phases of the project. Steve Ward taught us much of what we know about the intricacies of elastic layers and insisted on "minorizing before propagating," before we really understood why. Special thanks to all the folks of the Dead Lakes' Society. Reviews by Dick Peltier and two anonymous referees helped clarify the presentation of our results. Data acquisition and early stages of the modeling were supported by NSF grant EAR-8721114.

References

Argus, D.F., and R.G. Gordon, Current Sierra Nevada-North America motion from very long baseline interferometry: Implications for the kinematics of the western United States, *Geology, 19*, 1085-1088, 1991.

Ashby, M.F., and R.A. Verrall, Micromechanisms of flow and fracture, and their relevance to the rheology of the upper mantle, *Philos. Trans. R. Soc. London, Ser. A, 288*, 59-95, 1977.

Barazangi, M., and B.L. Isacks, Spatial distribution of earthquakes and subduction of the Nazca plate beneath South America, *Geology, 4*, 686-692, 1976.

Bard, E., B. Hamelin, R.G. Fairbanks, and A. Zindler, Calibration of the ^{14}C timescale of the past 30,000 years using mass spectrometric U-Th ages from Barbados corals, *Nature, 345*, 405-410, 1990.

Bechtel, T.D., D.W. Forsyth, V.L. Sharpton, and R.A.F. Grieve, Variations in effective elastic thickness of the North American lithosphere, *Nature, 343*, 636-638, 1990.

Beghoul, N., M. Barazanghi, and B.L. Isacks, Lithospheric structure of Tibet and western North America: Mechanisms of uplift and a comparative study, *J. Geophys. Res., 98*, 1997-2016, 1993.

Bills, B.G., and G.M. May, Lake Bonneville: Constraints on lithospheric thickness and upper mantle viscosity from isostatic warping of Bonneville, Provo, and Gilbert stage shorelines, *J. Geophys. Res., 92*, 11,493-11,508, 1987.

Bills, B.G., S.L. de Silva, D.R. Currey, R.S. Emenger, K.D. Lillquist, A. Donnellan, and B. Worden, Hydro-isostatic deflection and tectonic tilting in the central Andes: Initial results of a GPS survey of Lake Minchin shorelines, *Geophys. Res. Lett., 21*, 293-296, 1994.

Biot, M.A., Theory of stress-strain relations in anisotropic visco-elasticity and relaxation phenomena, *J. Appl. Phys., 25*, 1385-1396, 1954.

Bird, P., Formation of the Rocky Mountains, western United States: A continuum computer model, *Science, 239*, 1501-1507, 1988.

Borch, R.S., and H.W. Green, Dependence of creep in olivine on homologous temperature and its implications for flow in the mantle, *Nature, 330*, 345-348, 1987.

Brennen, C., Isostatic recovery and strain rate dependent viscosity of the Earth's mantle, *J. Geophys. Res., 79*, 3993-4001, 1974.

Brotchie, J.F., and R. Silvester, On crustal flexure, *J. Geophys. Res., 74*, 5240-5252, 1969.

Buck, W.R., Flexural rotation of normal faults, *Tectonics, 7*, 959-973, 1988.

Burgers, J.M., Mechanical considerations, model systems, phenomenological theories, in *First Report on Viscosity and Plasticity*, pp. 21-23, Akademie van Wetenshafen, Amsterdam, 1935.

Burr, T.N., and D.R. Currey, The Stockton Bar, edited by M.N. Machette, In the Footsteps of G.K. Gilbert–Lake Bonneville and Neotectonics of the Eastern Basin and Range Province. *Utah Geol. Miner. Surv. Misc. Publ., 88-1*, 66-73, 1988.

Cathles, L.M., *The Viscosity of the Earth's Mantle*, 386 pp., Princeton University Press, Princeton, N. J., 1975.

Chen, W., and P. Molnar, Focal depths of intracontinental and intraplate earthquakes and its implications for the thermal and mechanical properties of the lithosphere, *J. Geophys. Res., 88*, 4183-4214, 1983.

Condie, K.C., and C.K. Barsky, Origin of Quaternary basalts fro the Black Rock Desert region, Utah, *Geol. Soc. Am. Bull., 83*, 333-352, 1972.

Cost, T.L., Approximate Laplace transform inversions in visco-elastic stress analysis, *AIAA J., 2*, 2157-2166, 1964.

Crittenden, M.D., New data on the isostatic deformation of Lake Bonneville, *U.S. Geol. Surv. Prof. Pap., 454*, E1-E31, 1963a.

Crittenden, M.D., Effective viscosity of the Earth derived from isostatic loading of Pleistocene Lake Bonneville, *J. Geophys. Res., 68*, 5517-5530, 1963b.

Crittenden, M.D., Viscosity and finite strength of the mantle as determined from water and ice loads, *Geophys. J. R. Astron. Soc., 14*, 261-279, 1970.

Crough, S.T., Isostatic rebound and power-law flow in the asthenosphere, *Geophys. J. R. Astron. Soc., 50*, 723-738, 1977.

Currey, D.R., Lake Bonneville: Selected features of relevance to neotectonic analysis, *U.S. Geol. Surv. Open File Rep., 82-1070*, 31 pp., 1982.

Currey, D.R., Quaternary paleolakes in the evolution of semidesert basins, with special emphasis on Lake Bonneville and the Great Basin, *Palaeogeogr. Palaeoclimatol. Palaeoecol., 76*, 189-214, 1990.

Currey, D.R., and T.N. Burr, Linear model of threshold controlled shorelines of Lake Bonneville, in edited byM.N. Machette, In the Footsteps of G.K. Gilbert–Lake Bonneville and Neotectonics of the Eastern Basin and Range province, *Utah Geol. Miner. Surv. Misc. Publ., 88-1*, 104-110, 1988.

Currey, D.R., and C.G. Oviatt, Durations, average rates, and probable causes of Lake Bonneville expansions, stillstands, and contractions during the last deep-lake cycle, 32,000 to 10,000 years ago, *Geogr. J. Korea, 10*, 1085-1099, 1985.

Currey, D.R., C.G. Oviatt, and G.B. Plyler, Lake Bonneville stratigraphy, geomorphology, and isostatic deformation in west-central Utah, *Utah Geol. Miner. Surv. Spec. Stud., 62*, 63-82, 1983.

Currey, D.R., C.G. Oviatt, and J.E. Czarnomski, Late Quaternary geology of Lake Bonneville and Lake Waring, *Utah Geol. Assoc. Publ., 13*, 227-237, 1984.

Eardley, A.J., R.T. Shuey, V. Gvodetsky, W.P. Nash, M.D. Picard, D.C. Grey, and G.J. Kukla, Lake cycles in the Bonneville basin, Utah, *Geol. Soc. Am. Bull., 84*, 211-216, 1973.

Fletcher, R.C., and B. Hallet, Unstable extension of the lithosphere: A mechanical model for Basin and Range structure, *J. Geophys. Res., 88*, 7457-7466, 1983.

Forman, S.L., A.R. Nelson, andJ.P. McCalpin, Thermoluninescence dating of fault scarp derived colluvium: Deciphering the timing of paleoearthquakes on the Weber segment of the Wasatch fault zone, north central Utah, *J. Geophys. Res., 96*, 595-605, 1991.

Froidevaux, C., Basin and Range large scale tectonics: Constraints from gravity and reflection seismology, *J. Geophys. Res., 91*, 3625-3632, 1986.

Froidevaux, C., and B.L. Isacks, The mechanical state of the lithosphere in the Altiplano-Puna segment of the Andes, *Earth Planet. Sci. Lett., 71*, 305-314, 1984.

Gantmacher, F.R., *The Theory of Matrices*, Chelsea Pub. Co., New York, 1974.

Gilbert, G.K., Lake Bonneville, *U.S. Geol. Surv. Monogr., 1*, 438 pp., 1890.

Gilbert, F., and G. Backus, Propagator matrices in elastic wave and vibration problems, *Geophysics, 31*, 326-332, 1966.

Gittus, J., Creep, *Viscoelasticity and Creep Fracture in Solids*, Applied Science Publishers, London, 1975.

Hummel, W., and J. Arndt, Variation of viscosity with temperature and composition in the plagioclase system, *Contrib. Mineral. Petrol., 90*, 83-92, 1985.

Humphreys, E.D., and K.G. Dueker, Western U.S. upper mantle structure, *J. Geophys. Res., 99*, 9615-9634, 1994a.

Humphreys, E.D., and K.G. Dueker, Physical state of the western U.S. upper mantle, *J. Geophys. Res., 99*, 9635-9650, 1994b.

Isacks, B.L., Uplift of the Central Andean Plateau and bending of the Bolivian orocline, *J. Geophys. Res., 93*, 3211-3231, 1988.

Iwasaki, T., and M. Matsu'ura, Quasi-static crustal deformations due to a surface load, *J. Phys. Earth, 30*, 469-508, 1982.

Jordan, T.E., and J.N. Alonso, Cenozoic stratigraphy and basin tectonics of the Andes mountains, 20-28 south latitude, *AAPG Bull., 71*, 49-64, 1987.

Kerr, A.D., Elastic and viscoelastic foundation models, *J. Appl. Mech., 31*, 491-498, 1964.

Kirby, S.H., Rheology of the lithosphere, *Rev. Geophys., 21*, 1458-1487, 1983.

Kono, M., Y. Fukao, and A. Yamamoto, Mountain building in the Central Andes, *J. Geophys. Res., 94*, 3891-3905, 1989.

Kornig, M., and G. Muller, Rheological models and interpretation of postglacial uplift, *Geophys. J. Int., 98*, 243-253, 1989.

Kruse, S., M. McNutt, J. Phipps Morgan, L. Royden, and B. Wernicke, Lithospheric extension near Lake Mead, Nevada: A model for ductile flow in the lower crust, *J. Geophys. Res., 96*, 4435-4456, 1991.

Lachenbruch, A.H., Heat flow in the Basin and Range province and thermal effects of tectonic extension, *Pure Appl. Geophys., 117*, 34-50, 1978.

Lee, E.H., Stress analysis in viscoelastic bodies, *Q. Appl. Math., 13*, 183-189, 1955.

Love, A.E.H., *Some Problems of Geodynamics*, 180 pp., Cambridge University Press, New York, 1911.

Machette, M.N., S.F. Personius, A.R. Nelson, D.P. Schwartz, and W.R. Lund, The Wasatch Fault Zone, Utah: Segmentation and history of Holocene faulting, *J. Struct. Geol., 13*, 137-149, 1991.

May, G.M., B.G. Bills, and D.S. Hodge, Far-field flexural response of Lake Bonneville from paleopluvial lake elevations, *Phys. Earth Planet. Int., 68*, 274-284, 1991.

McAdoo, D.C., and D.B. Zilkowski, Apparent crustal motions in response to historical changes in the level of Great Salt Lake: Indicators of a weak lower crust, *Eos Trans. AGU, 67*, 1184, 1986.

McConell, R.K., Isostatic adjustment in a layered Earth, *J. Geophys. Res., 70*, 5171-5188, 1965.

McKee, E.H., and D.C. Noble, Tectonic and magmatic development of the Great Basin of western United States during late Cenozoic time, *Mod. Geol., 10*, 39-49, 1986.

Minster, J.B., and T.H. Jordan, Vector constraints on western U.S. deformation from space geodesy, neotectonics and plate motions, *J. Geophys. Res., 92*, 4798-4804, 1987.

Mitrovica, J.X., and W.R. Peltier, Free air gravity anomalies associated with glacial isostatic disequilibrium: Load history effects on the inference of deep mantle viscosity, *Geophys. Res. Lett., 18*, 235-238, 1991.

Mitrovica, J.X., and W.R. Peltier, A comparison of methods fro the inversion of viscoelastic relaxation spectra, *Geophys. J. Int., 108*, 410-414, 1992.

Morrison, R.B., Quaternary geology of the Great Basin, in *The Quaternary of the United States*, edited by H.E Wright and D.G. Frey, pp. 265-285, Princeton University Press, Princeton, N.J., 1965.

Morrison, R.B., Predecessors of Great Salt Lake, *Guideb. Utah Geol., 20*, 77-104, 1966.

Morrsion, R.B., Quaternary stratigraphic, hydrologic, and climatic history of the Great Basin, with emphasis on Lakes Lahontan, Bonneville, and Tecopa, in *Quaternary Nonglacial Geology; Conterminous U.S., The Geology of North America*, vol. K-2, pp. 283-320, Geological Society of America, Boulder, Colo., 1991.

Muller, G., Generalized Maxwell bodies and estimates of mantle viscosity, *Geophys. J. R. Astron. Soc., 87*, 1113-1141, 1986.

Nakiboglu, S.M., and K. Lambeck, A study of the Earth's response to surface loading with applications to Lake Bonneville, *Geophys. J. R. Astron. Soc., 70*, 577-620, 1982.

Nakiboglu, S.M., and K. Lambeck, A reevaluation of the isostatic rebound of Lake Bonneville, *J. Geophys. Res., 88*, 10,439-10,447, 1983.

Oviatt, C.G., Quaternary geology of the Black Rock Desert, Millard county, Utah, *Utah Geol. Miner. Surv. Spec. Stud., 73*, 27 pp., 1991.

Oviatt, C.G., and W.P. Nash, Late Pleistocene basaltic ash and volcanic eruptions in the Bonneville basin, Utah, *Geol. Soc. Am. Bull., 101*, 292-303, 1989.

Pan, E., Static response of a transversely isotropic and layered half-space to general surface loads, *Phys. Earth Planet. Inter., 54*, 353-363, 1989.

Passey, Q.R., Upper mantle viscosity derived from the difference in rebound of the Provo and Bonneville shorelines: Lake Bonneville basin, *J. Geophys. Res., 86*, 11,701-11,708, 1981.

Peltier, W.R., The impulse response of a Maxwell Earth, *Rev. Geophys., 12*, 649-669, 1974.

Peltier, W.R., New constraints on transient lower mantle rheology and internal mantle buoyancy from glacial rebound data, *Nature, 318*, 614-617, 1985.

Peltier, W.R., Deglaciation induced vertical motion of the North American continent and transient lower mantle rheology, *J. Geophys. Res., 91*, 9099-9123, 1986.

Peltier, W.R., P. Wu, and D.A. Yuen, The viscosities of the Earth's mantle, in *Anelasticity in the Earth, Geodyn. Ser.* vol. 5, edited by F.D. Stacey, M.S. Paterson, and A. Nicholas, pp. 59-77, AGU, Washington, D.C.1981.

Peltier, W.R., R.A. Drummond, and A.M. Tushingham, Postglacial rebound and transient lower mantle rheology, *Geophys. J. R. Astron. Soc., 87*, 79-116, 1986.

Priestley, K., J.A. Orcutt, and J.N. Brune, Higher-mode surface waves and structure of the Great Basin of Nevada and Western Utah, *J. Geophys. Res., 85*, 7166-7174, 1980.

Ranalli, G., and D.C. Murphy, Rheological stratification of the lithosphere, *Tectonophysics, 132*, 281-295, 1987.

Rundle, J.B. Viscoelastic crustal deformation by finite quasi-static sources, *J. Geophys. Res., 83*, 5937-5945, 1978.

Rundle, J.B., Static elastic-gravitational deformation of a layered half space by point couple sources, *J. Geophys. Res., 85*, 5355-5363, 1980.

Rundle, J.B., Some solutions for static and pseudo-static deformation in layered, nonisothermal, porous media, *J. Phys. Earth, 30*, 421-440, 1982.

Sabadini, R., D.A. Yuen, and P. Gasperini, The effects of transient rheology on the interpretation of lower mantle viscosity, *Geophys. Res. Lett., 12*, 361-364, 1985.

Savage, J.C., M. Lisowski, and W.H. Prescott, Strain accumulation in the Rocky Mountain states, *J. Geophys. Res., 90*, 10,310-10,320, 1985.

Savage, J.C., M. Lisowski, and W.H. Prescott, Strain accumulation across the Wasatch Fault near Ogden, Utah, *J. Geophys. Res., 97*, 2071-2083, 1992.

Schapery, R.A., Two simple approximate methods of Laplace tranform inversion for visco-elastic stress analysis, *Rep. SM 61-23*, Grad. Aeronaut. Lab. Calif. Inst. of Technol., Pasadena, 1961.

Schwartz, D.P., and K. Coppersmith, Fault behavior and characteristic earthquakes: Examples from the Wasatch and San Andreas fault zones, *J. Geophys. Res., 89*, 5681-5698, 1984.

Scott, W.E., W.D. McCoy, R.R. Shroba, and R. Meyer, Reinterpretation of the exposed record of the last two cycles of Lake Bonneville, western United States, *Quat. Res., 20*, 261-285, 1983.

Servant, M., and J.C. Fontes, Les lacs Quaternaires des hauts plateaux des Andes boliviennes, *Cah. ORSTROM, Ser. Geol., 10*, 9-23, 1978.

Sibson, R.H., Fault zone models, heat flow, and the depth destribution of earthquakes in the continental crust of the United States, *Bull. Seismol. Soc. Am., 72*, 151-163, 1982.

Singh, S.J., Static deformation of a multilayered half-space by internal sources, *J. Geophys. Res., 75*, 3257-3263, 1970.

Singh, S.J., Static deformation of a transversely isotropic layered elastic half-space by surface loads, *Phys. Earth Planet. Inter., 42*, 263-273, 1986.

Smith, B.K., and F.O. Carpenter, Transient creep in orthosilicates, *Phys. Earth Planet. Inter., 49*, 314-324, 1987.

Smith, R.B., and R.L. Bruhn, Intraplate extensional tectonics of the eastern Basin and Range: Inferences on structural style from seismic reflection data, regional tectonics, and thermal-mechanical models of brittle-ductile deformation, *J. Geophys. Res., 89*, 5732-5762, 1984.

Spencer, R.J., M.J. Baedecker, H.P. Eugster, R.M. Forester, M.B. Goldhader, B.F. Jones, K. Kelts, J. McKenzie, D.B. Madsen, S.L. Rettig, M. Rubin, and C.J. Bowser, Great Salt Lake and predecessors, Utah: The last 30,000 years, *Contrib. Minerer. Petrol., 86*, 321-334, 1984.

Stein, R.S., G.C.P. King, and J.B. Rundle, The growth of geologic structures by repeated earthquakes 2, Field ex-

amples of continental dip-slip faults, *J. Geophys. Res., 93*, 13319-13331, 1988.

Stewart, J.H., Regional tilt patterns of late Cenozoic basin-range fault blocks, western United States, *Geol. Soc. Am. Bull., 91*, 460-464, 1980.

Toscano, M.A., and L.L. York, Quaternary stratigraphy and sea-level history of the U.S. middle Atlantic coastal plain, *Quat. Sci. Rev., 11*, 301-328, 1992.

Tushingham, A.M., and W.R. Peltier, Ice-3G: A new global model of Late Pleistocene deglaciation based upon geophysical predictions of postglacial relative sea level change, *J. Geophys. Res., 96*, 4497-4523, 1991.

Tushingham, A.M., and W.R. Peltier, Implications of the radiocarbon timescale for ice-sheet chronology and sea-level change, *Quat. Res., 39*, 125-129, 1993.

Walcott, R.I., Flexural rigidity, thickness, and viscosity of the lithosphere, *J. Geophys. Res., 75*, 3941-3954, 1970.

Ward, S.N., A note on lithospheric bending calculations, *Geophys. J. R. Astron. Soc., 78*, 241-253, 1984.

Ward, S.N., Quasi-static propagator matrices: Creep on strike-slip faults, *Tectonophysics, 120*, 83-106, 1985.

Ward, S.N., Pacific-North America plate motions: New results from very long baseline interferometry, *J. Geophys. Res., 95*, 21,965-21,981, 1990.

Weertman, J., Creep laws for the mantle of the Earth, *Philos. Trans. R. Soc. London, Ser. A, 288*, 9-26, 1978.

Weijermars, R., and H. Schmeling, Scaling of Newtonian and non-Newtonian fluid dynamics without inertia for quantitative modelling of rock flow due to gravity, *Phys. Earth Planet. Inter., 43*, 316-330, 1986.

Wernicke, B.P., and G.J. Axen, On the role of isostacy in the evolution of normal fault systems, *Geology, 16*, 848-851, 1988.

Wolf, D., Thick-plate flexure re-examined, *Geophys. J. R. Astron. Soc., 80*, 265-273, 1985a.

Wolf, D., On Boussinesq's problem for Maxwell continua subject to an external gravity field, *Geophys. J. R. Astron. Soc., 80*, 275-279, 1985b.

Wu, P., and W.R. Peltier, Viscous gravitational relaxation, *Geophys. J. R. Astron. Soc., 70*, 435-485, 1982.

Wyman, M., Deflections of an infinite plate, *Can. J. Res., Ser. A 28*, 293-302, 1950.

Yechieli, Y., M. Magaritz, Y. Levy, U. Weber, and G. Bonani, Late quaternary geological history of the Dead Sea area, Israel, *Quat. Res., 39*, 59-67, 1993.

Zoback, M.L., State of stress and modern deformation of the northern Basin and Range province, *J. Geophys. Res., 94*, 7105-7128, 1989.

Zoback, M.L., R.E. Anderson, and G.A. Thompson, Cainozoic evolution of the state of stress and style of tectonism of the Basin and Range province of the western United States, *Philos. Trans. R. Soc. London Ser. A, 300*, 407-434, 1981.

Zuber, M.T., E.M. Parmentier, and R.C. Fletcher, Extension of continental lithosphere: A model for two scales of Basin and Range deformation, *J. Geophys. Res., 91*, 4826-4838, 1986.

B.G. Bills, Geodynamics Branch, Code 921, NASA Goddard Space Flight Center, Greenbelt, MD 20771. (e-mail: bills@denali.gsfc.nasa.gov)

D.R. Currey, Limneotectonics Laboratory, Department of Geography, University of Utah, Salt Lake City, UT 84112.

G.A. Marshall, Branch of Earthquake Geology and Geophysics, MS 977, U.S. Geological Survey, 345 Middlefield Road, Menlo Park, CA 94025.

(Received September 17, 1992; revised April 29, 1994; accepted May 3, 1994.)